European Journal of Medicinal Chemistry 74 (2014) 199–215

Contents lists available at ScienceDirect

European Journal of Medicinal Chemistry

journal homepage: http://www.elsevier.com/locate/ejmech

Original article

Syntheses and evaluation of drug-like properties of CO-releasing molecules containing ruthenium and group 6 metal

Pengpeng Wang [a], Huapeng Liu [a], Quanyi Zhao [a,*], Yonglin Chen [b], Bin Liu [c], Baoping Zhang [c], Qian Zheng [c]

[a] Institute of Medicinal Chemistry, School of Pharmacy of Lanzhou University, Lanzhou, PR China
[b] The First Affiliated Hospital of Lanzhou University, Lanzhou, PR China
[c] School of Stomatology of Lanzhou University, Lanzhou 730000, PR China

ARTICLE INFO

Article history:
Received 18 July 2013
Received in revised form
24 December 2013
Accepted 26 December 2013
Available online 9 January 2014

Keywords:
CO-releasing molecules
Toxicity
Distribution
Metabolism
Drug-like properties

ABSTRACT

In this paper, drug-like properties of two series of carbonyl metal CO-releasing molecules, $Ru(CO)_3Cl_nL$ ($n = 1$, L = amino acid or its derivatives **1**–**7**, L = acetylacetone **8** or 2,2′-bipyridyl **9**; $n = 2$, L = aminopyridine derivatives **10**–**13**; $n = 0$, L = salicylaldehyde Schiff base **14**–**15**) and $M(CO)_5L$(M = Cr, Mo, W; L = glycine methyl ester **16**–**18**; L = N-methyl imidazole **19**–**21**), were preliminarily evaluated from four aspects involving in cytotoxicity, *in vivo* toxicity, bio-distribution and metabolism. Cytotoxic effects of all complexes were assayed by MTT. IC_{50} values of complexes **1**–**15** were 39.55–240.16 mg/l, and those of complexes **16** and **18** were 21.36–22.21 mg/l. Toxicity tests of mice used oral acute toxic class method and got LD_{50} values of some complexes; among them, LD_{50} of complex **1** was in 800–1000 mg/kg, complex **7** in 1100–1500 mg/kg and complex **18** in 75–125 mg/kg. After several consecutive administrations, tested complexes severely damaged liver and kidney in both functional and morphological aspects. And by metal ions measurements using ICP-AES, we found that the tested complexes were unevenly distributed in tissues and organs. *In vivo*, Ru^{II} in complexes was oxidized to Ru^{III} by P450 enzymes, and for Mo^0 and W^0 in complexes, part of them transformed into higher oxidation state, the others kept original state.

1. Introduction

Like nitric oxide, carbon monoxide (CO) is an important yet only recently recognized biological signaling molecule [1]. CO is generated endogenously through catabolism of Heme, which is catalyzed by heme oxygenases. It exhibits cytoprotective, anti-inflammatory, vasodilatory and other beneficial effects [2]. However, the application of CO as a therapeutic agent is still in its infancy [3,4]. The use of gaseous CO is risky and limited because of its low bioavailability and high affinity toward hemoglobin which resulting systemic effects on oxygen transport [5]. The use of CO-releasing molecules (CORMs) instead of gaseous CO is a promising strategy to deliver controlled amounts of CO directly to the tissue or organ. The vast majority of CORMs takes advantage of the well known affinity of transition-metal complexes for CO, although a boron-based CORM has also been employed [6–8] and it has been shown that organic compounds such as CH_2Cl_2 may also act as sources of carbon monoxide [5].

In this field, R. Motterlini and co-workers are pioneers who have identified a series of transition-metal carbonyl complexes that fulfilled this function [9–11]. While the early CORMs, such as $[Mn_2(CO)_{10}]$, needed UV activation; and $[Ru(CO)_3Cl_2]_2$ releases CO accompanying with ligand exchange with DMSO [12]. The related mononuclear glycinato complex *fac*-$[Ru(CO)_3Cl(NH_2CH_2COO)]$ is more soluble in water and releases CO under physiological conditions [13]. However, CO release from *fac*-$[Ru(CO)_3Cl(NH_2CH_2COO)]$ is very fast and unspecific [14], which hampers the delivery of controlled amounts of CO to a target tissue. To overcome this problem, Steffen Romanski used enzyme-trigger to control the rate of CO release from acyloxybutadiene iron tricarbonyl complexes [15], while other researchers also achieved this goal by pH-dependent CO liberation [6,8] or photo-induced CO releasing [16–20]. Meanwhile, to minimize potential toxic side effects, some biologically compatible ligands such as amino acids [21–24], sugars [25,26], and 2-pyrone motif [27,28], were introduced into structures of CORMs to get a kind of drug-like molecules. In another aspect, many metals with a defined biological role such as iron [23,24,27–35], manganese [36–43], and molybdenum [22,28,31] were the first choices to think over. However, this has not

* Corresponding author. Tel./fax: +86 931 891 5686.
E-mail address: zhaoqy@lzu.edu.cn (Q. Zhao).

0223-5234/$ – see front matter © 2014 Elsevier Masson SAS. All rights reserved.
http://dx.doi.org/10.1016/j.ejmech.2013.12.041

precluded the use of a wide range of metals which have no, or little, intrinsic biological role, notably with ruthenium in CORMs [21] as well as chromium- [22,31], tungsten- [18,22,31], rhenium- [41,44–46], cobalt-, and iridium-based [47] systems being developed. Among these compounds, only a part of them were tested in various biological assays, and promising activities were documented, and preclinical studies are in progress [7,9–11].

Though many CORMs have been synthesized and identified, so far, little is known about the metabolic fate of complexes after CO release except that only a few of them have been revealed their abilities to enter cells [16,36,48,49], combine with proteins [50,51] and cytochromes [52], certainly nor are their pharmacokinetic and metabolic properties, including their reaction products formed *in vitro* and *in vivo*. Without further biological investigation it will not be known if these CORMs have value in medicine.

Therefore, based on the syntheses of two series of CORMs, we mainly investigated their drug-like properties in this paper, not only involving CO-releasing half-life, cell toxicity, mice toxicity, but also liver and kidney toxicity. Furthermore, we also preliminarily investigated the distribution of CORMs in main tissues and organs, and traced the metabolic process of complexes using many tools such as XPS, FT-IR. By which we hope to get some information about whether these carbonyl metal complexes have value in medicine really, and how to set a quality standard and develop a suitable pharmaceutical formulation.

2. Results and discussions

2.1. Syntheses, characterization and properties

Syntheses of carbonyl ruthenium complexes **1**–**15** commenced from reagent ruthenium trichloride hydrate and commercially available formic acid via reduction reaction to get $[Ru(CO)_3Cl_2]_2$. Then $[Ru(CO)_3Cl_2]_2$ reacted with amino acids or their derivatives to get complexes **1**–**7**, with acetylacetone to get complex **8**, with 2,2′-bipyridyl to get complex **9**, with aminopyridine derivatives to get complexes **10**–**13** and with salicylaldehyde Schiff base to get complex **14**, **15** (Scheme 1). Syntheses of group 6 CO-releasing metal complexes **16**–**21** used intermediate $[NEt_4][MCl(CO)_5]$ that was accessed via the reaction of NEt_4Cl with $M(CO)_6$ in higher boiling point solvent, then by ligand exchange reaction to get the goal molecules (Scheme 2). All ruthenium complexes were obtained in moderate to good yields. They are powder solids from white-yellow to yellow and stable even if exposed to light and air, which was confirmed by NMR spectroscopy and elemental analysis. Complexes **1**–**4** dissolve easily in water and their aqueous solutions are acidic, which are consistent with reports in literatures [13,21]. Acid and base, even some solvents, can affect their properties. Other ruthenium complexes **5**–**15** have poor water-solubility, and can dissolve in organic solvents, such as DMSO, methanol, DCM. As for complexes **16**–**21**, they are stable in air, but sensitive to light so that a part of them decomposed during the course of purification. Among them, complexes containing glycine methyl ester ligand have better water-solubility than others having *N*-methyl imidazole ligand, and all of them can dissolve in organic solvents like DCM and THF. All synthesized complexes were characterized by standard methods (see Experimental Section).

The structure of CORMs may be divided into two parts (Fig. 1), one is carrier and another is CO molecule for functional group. In carrier part, metal atom acts as action of immobilization by coordination bond and makes gaseous CO molecule transform into solid state which can be easily controlled in dose; non-CO ligands do not affect the function of CORMs, just modulate the properties of the whole molecule, such as molecular polarity and stability in solutions.

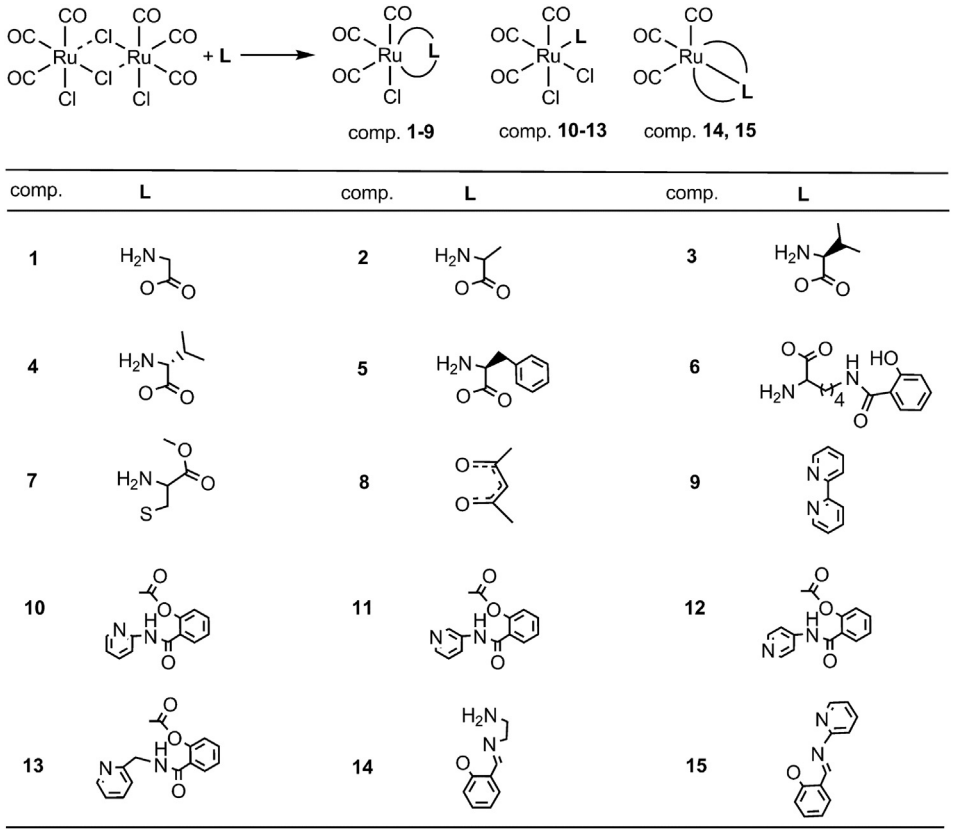

Scheme 1. Syntheses and structures of CORMs containing Ru^{II} atom.

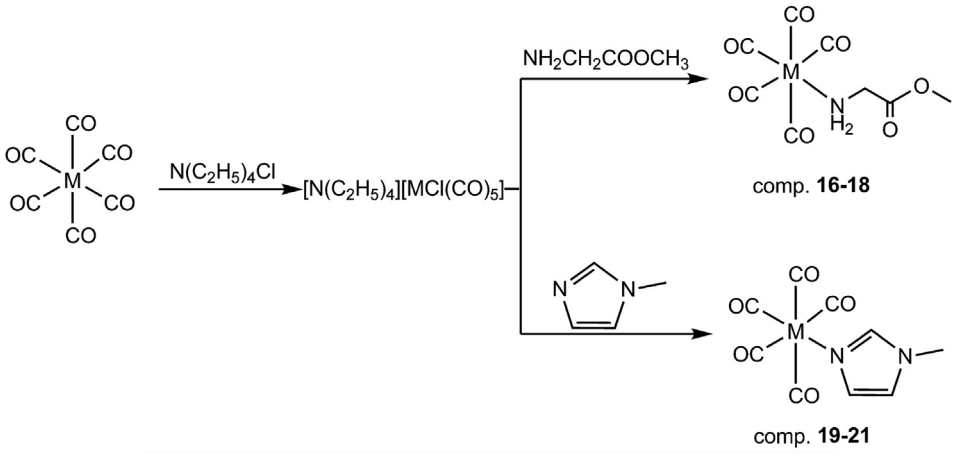

comp.	M	comp.	M	comp.	M
16	Cr	**17**	Mo	**18**	W
19	Cr	**20**	Mo	**21**	W

Scheme 2. Syntheses and structures of CORMs containing Cr, Mo, W atom.

Amino acid is used as bidentate ligand because of lower toxicity, such as one typical complex *fac*-[$Ru(CO)_3Cl(NH_2CH_2COO)$]; but this complex featuring an O, N-chelating motif and a halido ligand often has several forms resulting from the ligand exchange reaction in solution [13].

The hydrophobicity of a molecule is measured by its log *P* value. In order to accurately evaluate these complexes' capability of crossing membrane, we used phosphate buffer (0.1 M, pH = 7.4) instead of water to measure their log *P* values (Table 1). Seen from the data, all log *P* values are small; besides ligands, metal ions also have a certain effect on the log *P* values; among complexes **16**–**18**, complex **17** has a more polarity than the other two under the same ligand condition.

The release of CO from CORMs can be monitored spectrophotometrically [53]. Deoxy myoglobin (deoxy-Mb) has a high affinity for CO, and it can bind one CO to form carbonyl myoglobin (CO-Mb). The difference between absorption maxima of deoxy-Mb and CO-Mb allows detection of the CO released from CORMs. This method was applied to study the CO releasing ability of CORMs. To evaluate both the total amount of CO released and its rate of release, complexes were tested in three different concentrations (20, 40, 60 μM) following the changes in absorption. Some representative examples of the electronic spectrum are given in Fig. 2 (Others see SI-Fig. 1). All tested complexes were found to release CO and their rates of release were determined from 60 μM solution, the half-lives are given in Table 1 (Others see SI-Table 1). The studied complexes are effective releasers with half-lives varying between 1.0 min and 15.8 min. The differences in ligands within the series have certain effects on the CO release. When complexes **1**–**3** containing amino acid ligands compared with complexes **10** and **14** with aminopyridine derivative or Schiff base ligands, the former proved to be slightly faster releasers. In addition, the type of metal atom in complexes also has a certain effect on the rate of release, complexes **16**–**18** are all slower releasers, but their half-lives are increasing in the order of Mo < W < Cr.

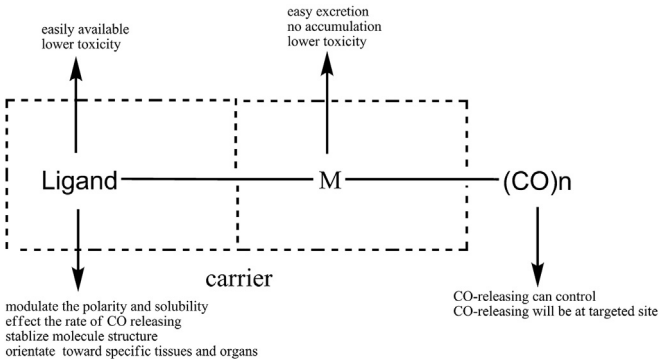

Fig. 1. The basic feature of carbonyl metal CO-releasing molecules.

2.2. Toxicity of carbonyl metal CO-releasing molecules

2.2.1. Cytotoxicity and toxicity in vivo

It was reported the toxicity of *fac*-[$Ru(CO)_3Cl(NH_2CH_2COO)$] is low, with a dose of 4 mg/kg for 30 days producing no adverse response in cynomolgus monkeys [54]. However, how much is the

Table 1
Log *P* values and CO-releasing half-lives of some complexes.

Comp.	Molecular formula	CO-releasing $t_{1/2}$ (min)	log *P*[a]
1	$[Ru(CO)_3Cl(NH_2CH_2COO)]$	4.9	−1.45
2	$[Ru(CO)_3Cl(NH_2CH(CH_3)COO)]$	3.2	−1.59
3	$[Ru(CO)_3Cl(NH_2CH(COO)CH(CH_3)_2)]$	1.1	−0.74
5	$[Ru(CO)_3Cl(NH_2CH(COO)CH_2C_6H_5)]$	1.6	−0.53
7	$[Ru(CO)_3Cl(NH_2CH(CH_2S)COOCH_3)]$	10.6	0.20
8	$[Ru(CO)_3Cl(CH_3COCHCOCH_3)]$	2.6	0.03
9	$[Ru(CO)_3Cl(2,2'\text{-bipyridyl})]$	13.2	−0.75
10	$[Ru(CO)_3Cl_2\mathbf{L_3}]$	10.6	−0.09
14	$[Ru(CO)_3\mathbf{L_7}]$	15.8	1.13
16	$[Cr(CO)_5(NH_2CH_2COOCH_3)]$	15.5	0.26
17	$[Mo(CO)_5(NH_2CH_2COOCH_3)]$	8.5	−0.61
18	$[W(CO)_5(NH_2CH_2COOCH_3)]$	13.9	−0.30

[a] The log *P* values are limited to accurately illustrate their ability to cross membranes, because the way of CORMs entering cells may not be free diffusion alone.

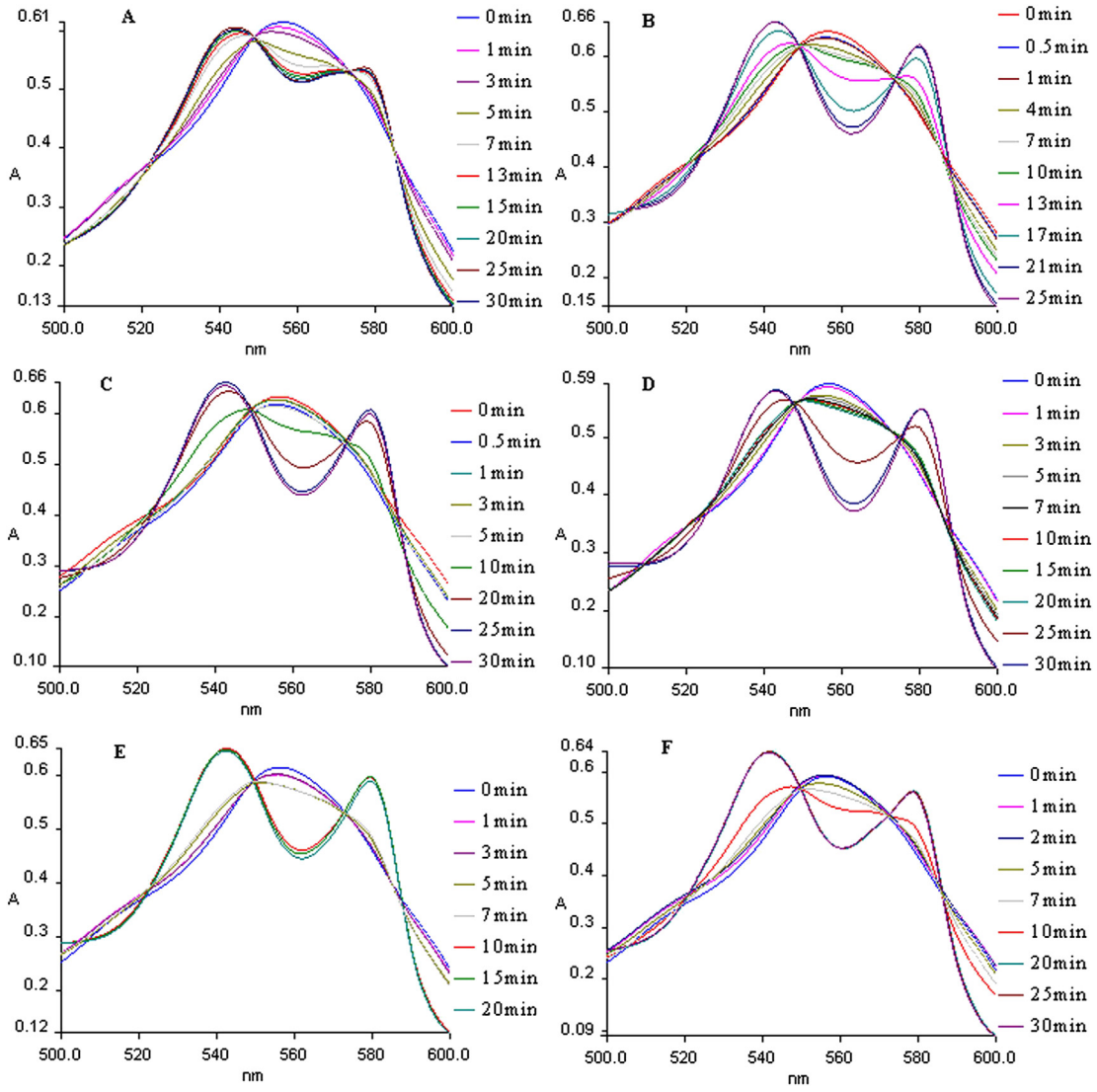

Fig. 2. The typical changes in the electronic spectrum of myoglobin as CO releasing from complexes (myoglobin binds one CO molecule to form carbonyl myoglobin). A, complex **1**; B for **7**; C for **10**; D for **14**; E for **17**; F for **19**.

minimum dose leading to toxic effects? What is IC_{50} for cells and LD_{50} for animals? In order to completely evaluate toxic effects of carbonyl metal CO-releasing molecules like *fac*-$[Ru(CO)_3Cl(NH_2CH_2COO)]$, and make sure that the toxicity is direct toxic effect or delayed toxic effect, the work was carried out in three aspects, cytotoxicity, toxicity *in vivo* and toxicity of complexes after several consecutive administrations.

The cytotoxic effects of complexes on the proliferation of fibroblast cells line were assayed by MTT. The tested concentrations were 100 μM, 200 μM, 400 μM, 800 μM and 1600 μM respectively. The results reveal that every ruthenium^{II} complex showed a very low antiproliferative activity. IC_{50} of complex **1** is 62.69 mg/l, and complex **7** 240.16 mg/l, showing a lower cytotoxicity. Among complexes **1**–**18** (SI-Table 2, SI-Fig. 2), IC_{50} values of complexes **3**–**5** are 5–6 times as high as that of complex **1**, and complex **9** is lower than that, this suggests that complexes **3**–**5** have much lower toxicity to fibroblast cells when compared with complex **1**, while complex **9** has higher toxicity. In addition, we noticed all the complexes containing Cr and W atom showed higher toxicity than every complex containing ruthenium atom, for example, complexes **16** and **18**, their IC_{50} values are 22.31 mg/l and 21.36 mg/l respectively.

Based on the cytotoxicity data of all complexes, 8 complexes were chosen to further assay their toxic effects through oral administration. To reduce the use of animals, we used the oral acute toxic class method (ATC method) [55] which was developed as an alternative to replace the oral LD_{50} test and obtained the range of LD_{50} values (Table 2). LD_{50} values of complexes **1** and **8** are in the same range of 800–1000 mg/kg, complexes **7** and **14** in the range of 1100–1500 mg/kg; among 5 complexes containing ruthenium, LD_{50} value of complex **10** is the smallest and only in the range of 150–200 mg/kg, which can be responsible for its higher toxicity. Complexes **16**–**18**, their LD_{50} values are 150–200 mg/kg, 300–500 mg/kg and 75–125 mg/kg respectively. These results are in accordance with those obtained from cells assay.

2.2.2. Toxicity of complexes after several consecutive administrations

In order to evaluate the toxicity of complexes after several consecutive administrations, rats were administered i.p. in a dose of 0.05–0.125 mmol per kilogram of body weight. These doses were selected in dependence on their effective and cytotoxic data. In 8–21 days later, the assays of the whole bloods were carried out to

Table 2
IC_{50} and LD_{50} values of some complexes.

Comp.	Molecular formula	IC_{50} (mg/l) fibroblast	LD_{50} (mg/kg) mice (oral)
1	$[Ru(CO)_3Cl(NH_2CH_2COO)]$	62.69	800–1000
7	$[Ru(CO)_3Cl(NH_2CH(CH_2S)COOCH_3)]$	240.16	1100–1500
8	$[Ru(CO)_3Cl(CH_3COCHCOCH_3)]$	70.16	800–1000
10	$[Ru(CO)_3Cl_2\mathbf{L_3}]$	39.55	150–200
14	$[Ru(CO)_3\mathbf{L_7}]$	255.48	1100–1500
16	$[Cr(CO)_5NH_2CH_2COOCH_3]$	22.31	150–200
17	$[Mo(CO)_5NH_2CH_2COOCH_3]$	194.02	300–500
18	$[W(CO)_5NH_2CH_2COOCH_3]$	21.36	75–125

analyze tested complexes' side-effects for liver function. The data of the bloods show that AST and ALT rise distinctly compared with the control group (SI-Table 3), especially complexes **17** and **18**, the measured values of AST are about 100 U/l higher than that of the control, and the measured values of ALT are about 20–30 U/l higher than the control. For complex **7**, both values are equal to the control. As complexes **1** and **16** are concerned, the values of AST increase by 50 U/l, but the values of ALT change a little. But unpredictably, the amounts of total proteins in blood almost keep unchanging for all tested complexes after several consecutive administrations; and the other assay indicators have no obvious difference from those of the control. However, through TEM, the morphological liver cells were seen in many kinds of abnormal states. There are many cells with karyopyknosis or chromatin margination, as well as those with slight expansion of mitochondria or cell nucleus deformity (Fig. 3). These disclose that the tested complexes damaged liver, and destroyed their cells.

Meanwhile, from the TEM results we could see some kidney cells were abnormal, and some damages were severe (Fig. 4). Morphologically, some kidney cells appeared either karyopyknosis, or nucleus deformity, or glomerular podocyte nuclei deformity, or hyperplasia of glomerular mesangial matrix, or podocyte foot process fusion, or even basement membrane rupture and glomerular capillary basement membrane collapse. In addition, by the inspection of urines, we found that urines were with proteins and their amounts were much more (SI-Table 4), this further suggested that tested carbonyl metal complexes severely affected functions of the kidney.

Therefore, seeing as a whole, these CORMs have side-effects on liver and kidney of tested rats. They have a little effect on the function of liver, but damage liver cells physiologically. More importantly, these complexes severely affect kidney in both functional and physiological aspects. Maybe, metal accumulation is one of reasons to give rise to side-effects.

2.3. Tissue absorption and distribution of complexes in vivo

In an attempt to further understand the *in vivo* toxicity of CORMs, some complexes were subjected to tissue distribution studies in mice. Animals were injected i.v. or i.p. with 0.25 mmol/kg of each complex in separate animals and were sacrificed from 10 min to 480 min thereafter, at each point the various tissues were collected and prepared for metal ions measurements using ICP-AES. Complexes first were absorbed into blood, then into tissues and organs. However, this does not mean even distribution around the body as some parts of the body have a richer blood supply than others.

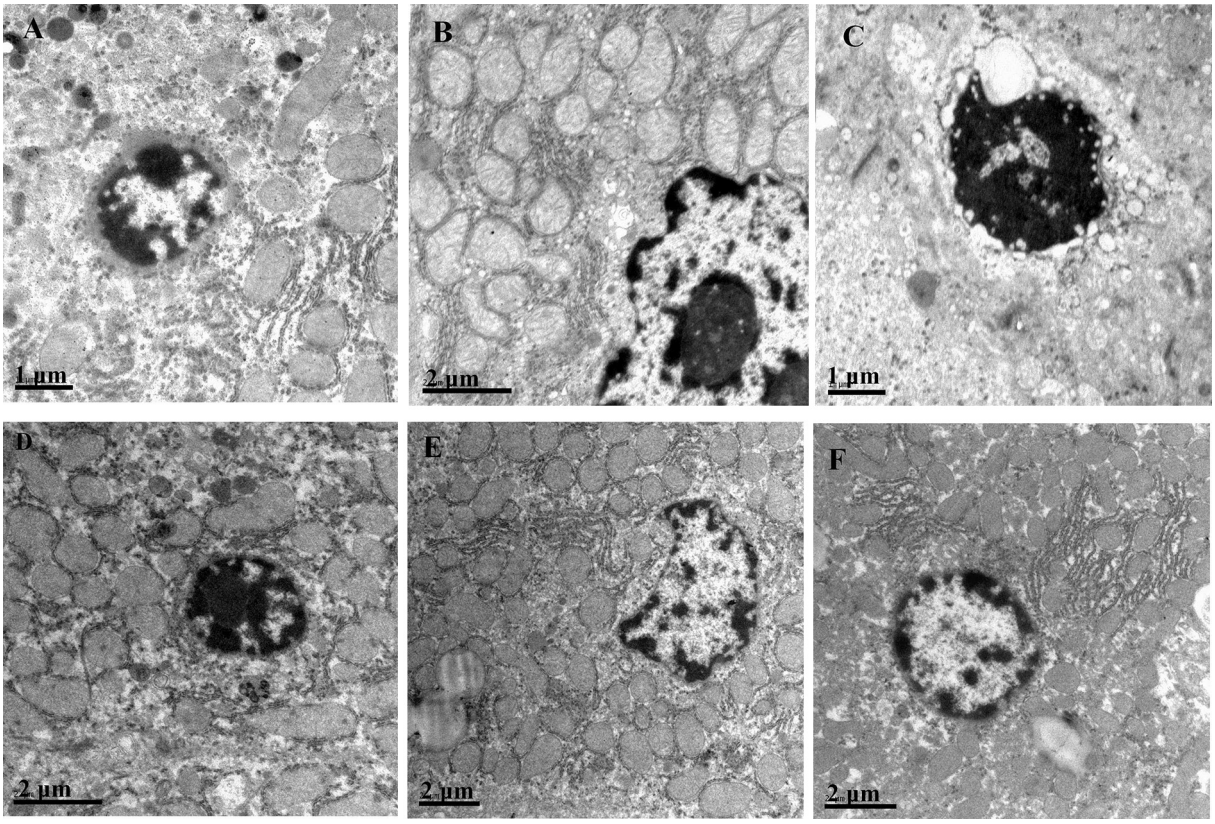

Fig. 3. TEM morphological images of liver cells from tested Wistar rats. Toxic effects of complexes appeared after administrating a certain dose successively 8–21 days. The morphological liver cells are seen in different states. For complex **1**: karyopyknosis and chromatin margination (A, 20,000-fold); complex **7**: slight expansion of mitochondria in liver cell (B, 15,000-fold) and karyopyknosis for liver cell (C, 15,000-fold). For **16**: karyopyknosis for liver cell (D, 15,000-fold); cell nucleus deformity (E, 10,000-fold) for **17** and chromatin margination for liver cell (F, 12,000-fold) for **18**.

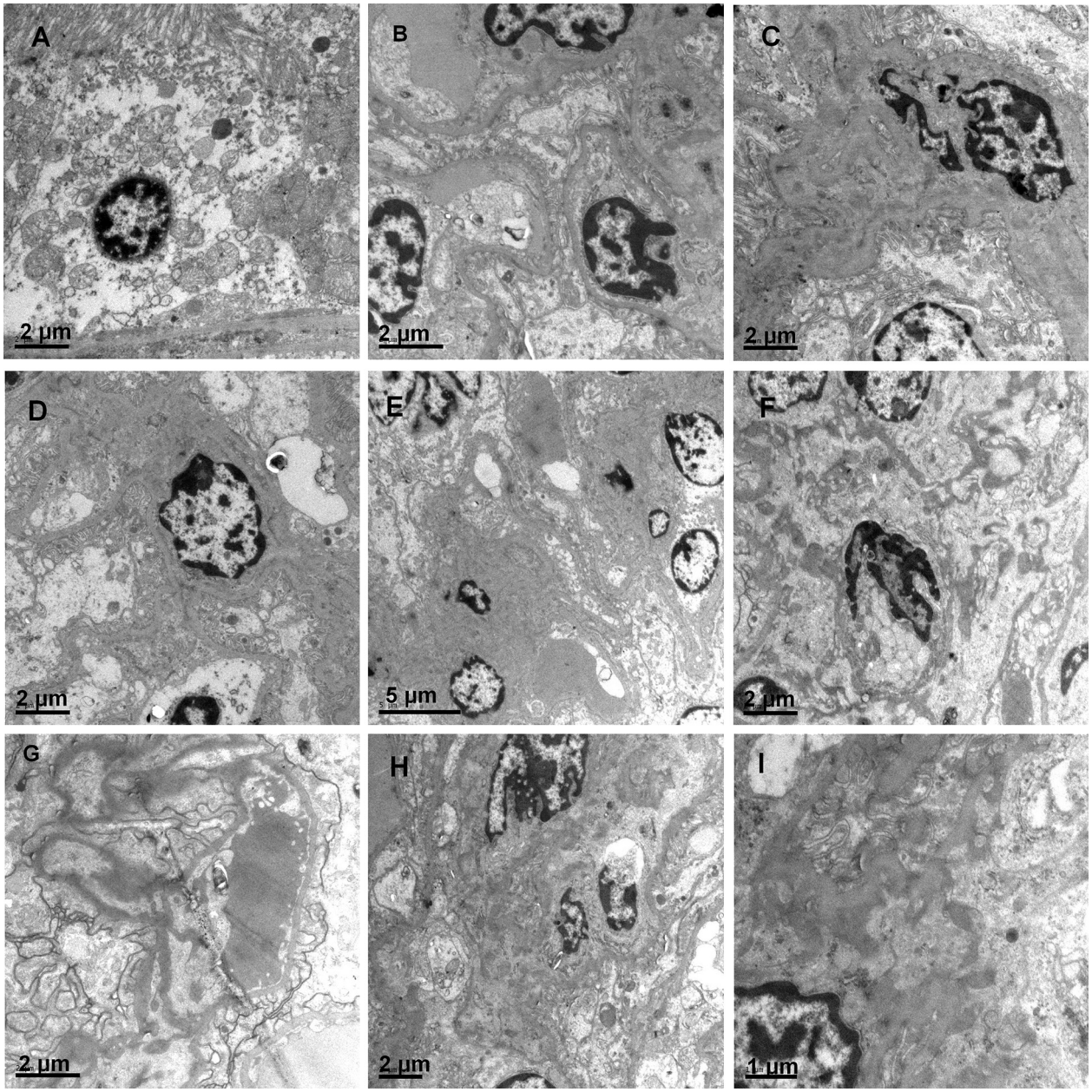

Fig. 4. TEM morphological images of kidney cells from tested Wistar rats. Toxic effects of complexes appeared after administrating a certain dose successively 8–21 days. The morphological kidney cells are seen in many states. For complex **1**: karyopyknosis (A, 10,000-fold); **7**: kidney cell nucleus deformity, proliferation of mesangial matrix (B, 12,000-fold and C, 10,000-fold); **16**: glomerular podocyte nuclei deformity, foot process fusion (D, 10,000-fold), and hyperplasia of glomerular mesangial matrix, podocyte foot process fusion (E, 6000-fold); **17**: hyperplasia of glomerular mesangial matrix, basement membrane rupture (F, 10,000-fold) and glomerular capillary basement membrane collapse, epithelial cell foot process fusion, luminal occlusion (G, 12,000-fold); **18**: glomerular capillary basement membrane collapse, epithelial cell foot process fusion, luminal occlusion (H, 8000-fold and I, 20,000-fold).

Among all CORMs, *fac*-[$Ru(CO)_3Cl(NH_2CH_2COO)$] is one of the most interesting complexes [2], so it is the first choice for us to figure out its *in vivo* dynamic properties. To evaluate the *in vivo* distribution of complex **1** as comprehensively and completely as possible, the ruthenium concentrations in blood, liver, kidney, lung, heart, spleen and brain were measured respectively after 10–60 min i.v. administered. The results show that the major proportion of complex **1** remains in blood (Fig. 5A). At the point of 10 min, it accounts for 11.46% in blood, 2.89% in liver, 6.85% in kidney, 2.25% in lung, 0.95% in heart and less than 0.5% in spleen and brain; In 30 min later it accounts for 8.99% in blood, 2.43% in liver, 3.09% in kidney, 0.87% in lung, 0.34% in heart and less than 0.5% in spleen and brain; After administered 60 min later, it accounts for 7.54% in blood, 2.23% in liver, 4.16% in kidney, 1.45% in lung, 0.46% in heart and less than 0.25% in spleen and brain. Apparently its amount in every organ and tissue changed with time, and blood, liver, kidney are main tissue and organ in which it collected; there is almost none in brain and spleen. In a word, distribution and metabolism of complex **1** are slow, and it can not cross the blood–brain barrier.

The properties of complexes determine their rates and extents of absorption and distribution. Complex **8** is insoluble in water, and it was administered by water–DMSO mixed solvent. Seen from Fig. 5B, after 30 min i.p. administered, the amount of complex **8** in

liver had arrived at a higher level and accounted for 8.01%, and in kidney 3.76%; and in 90 min later, the content of complex **8** in blood, liver and kidney was 4.12%, 4.96% and 4.64% respectively, and in lung 0.92%, spleen 1.06%, heart 0.30% and brain 0.08%. Compared with complex **1**, more amounts of complex **8** were in lung and spleen at the same point of time, and less amounts entered brain.

Just like an ordinary drug molecule, the hydrophobicity of a CORM has a close relation with its absorption and distribution. Though we do not know these molecules how to cross cell membranes at present, log *P* values are still important parameter to evaluate their properties. From Table 1, we can see a major proportion of complexes have a low log *P* value. This can interpret why they have almost no possibilities to cross the blood–brain barrier and the amounts of which penetrating into brain are very low.

Besides log *P* values, non-CO ligand is one of main factors responsible for their dynamic properties. Complex **1** has typical O, N bidentate ligand from glycine. After 30 min i.p. administered, only 0.26% of it appeared in blood, 0.43% entered liver and 0.37% in kidney, until 120 min, the concentration of blood approached climax and its amount accounted for 3.28%, distinctly its absorption is slow; at the same time, the amount in kidney also arrived in climax (Fig. 6A), but 240 min later, the amount of it in liver approached climax and accounted for 5.40%. Compared with complex **1**, the climax concentration of complex **7** containing N, S bidentate ligand in kidney appeared only after 30 min i.p. administered, and its amount accounted for 3.36%, and it was 120 min later that the concentration in liver approached climax and its amount accounted for 6.78%; And 480 min later, most of it excreted from kidney and entered urine (Fig. 6B). In brief, the absorption, distribution and metabolism of complex **7** are fast. In addition, complex **10** (Fig. 6C), the amount in liver was always higher than that in blood and kidney, after 120 min later its amount in liver accounted for 6.55%, but 240 min later, it decreased to 5.19%. Complex **14** was absorbed so slow that its concentration of blood still increased after administered 480 min. The majority was distributed in liver, and the amount in liver decreased gradually from 10.92% to 9.78%; similarly, the amount in kidney also decreased gradually from 2.25% to 1.58%. The amount in liver was about 5-fold as much as that in kidney (Fig. 6D). Complexes **16**–**18** have similar structures except for metal atom, but complex **16** was absorbed and distributed faster than both complexes **17** and **18**.

Interestingly, it was found that complex **8** was prone to stay in blood, complex **14** and complex **9** easily collected in liver; and complex **10** easily collected in kidney (SI-Fig. 3). But as for complexes **1**–**3** containing amino acid ligand, they were almost evenly distributed in blood, liver and kidney. And complexes containing ruthenium entered kidney more easily than those containing Cr, Mo, W atom.

In addition, some components in blood can affect the absorption and distribution of complexes. These substances mainly contain plasma proteins, glutathione, nucleoside, sugars and so on. *Fac*-$[Ru(CO)_3Cl(NH_2CH_2COO)]$ with various proteins can form protein–$Ru^{II}(CO)_2$ adducts [50]. This rapid formation of protein–$Ru^{II}(CO)_2$ adducts lowed the level of free complex. CO-releasing molecules $[Ru(CO)_3$(thiazole derivative)] reacted not only with the transport proteins, bovine serum albumin (BSA) and human apotransferrin (HTF), but also reacted with calf thymus DNA (CT-DNA) and guanosine-5′-monophosphate (GMP) at a lower extent [56]. As the plasma proteins cannot leave the capillaries, a complex bound to these proteins is also confined to the capillaries and cannot reach its target. And this binding is irreversible because both of them form a new and stable macromolecule through reaction. Our experimental results showed over 50% complexes **1** and **2** bound with plasma proteins after adding them into the whole blood of rat (Fig. 7); the amounts of which entering red cell accounted for about 20%, and increased with time; only less than 20% stayed in serum, and their amounts decreased with time.

2.4. Metabolism of CORMs

Possibly, complexes taken through i.v. or i.p. are absorbed into blood; then pass through liver before they proceed round the body. In plasma, some complexes will be hydrolyzed and some release CO ligand to form new complexes. In liver, every metal may be oxidized or reduced by P450 enzymes, all CO ligands replaced by other ligands such as H_2O, glutathione and active endogenous substances; then the first metabolites enter kidney. In order to get the information of metabolites of complexes, the urines from CORMs treated rats were collected and treated (SI-Table 5).

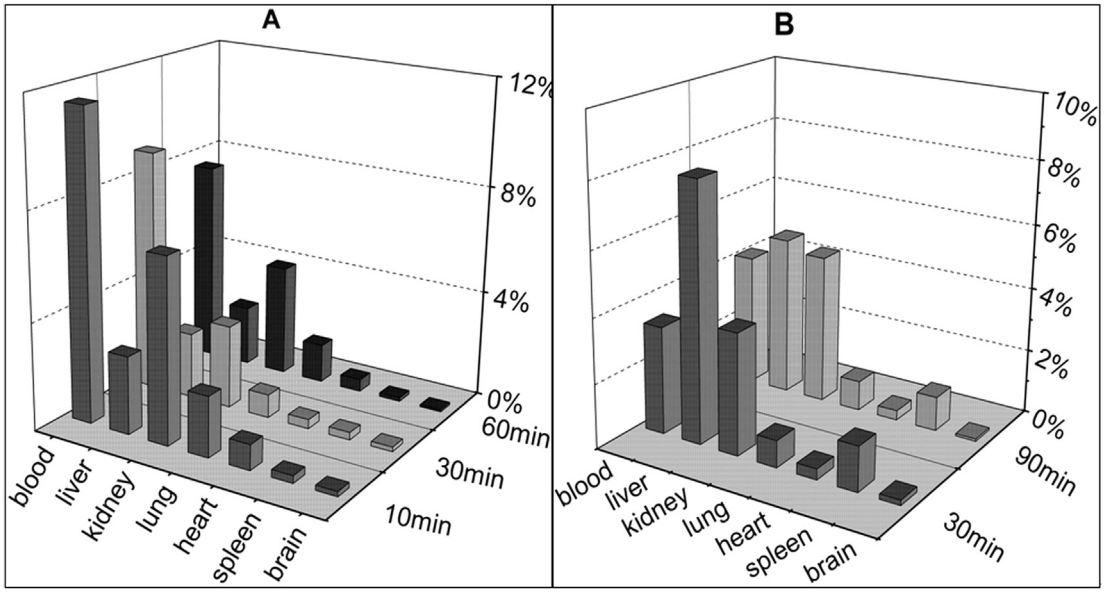

Fig. 5. Distribution of complex **1**(A) and **8**(B) in organs and tissues.

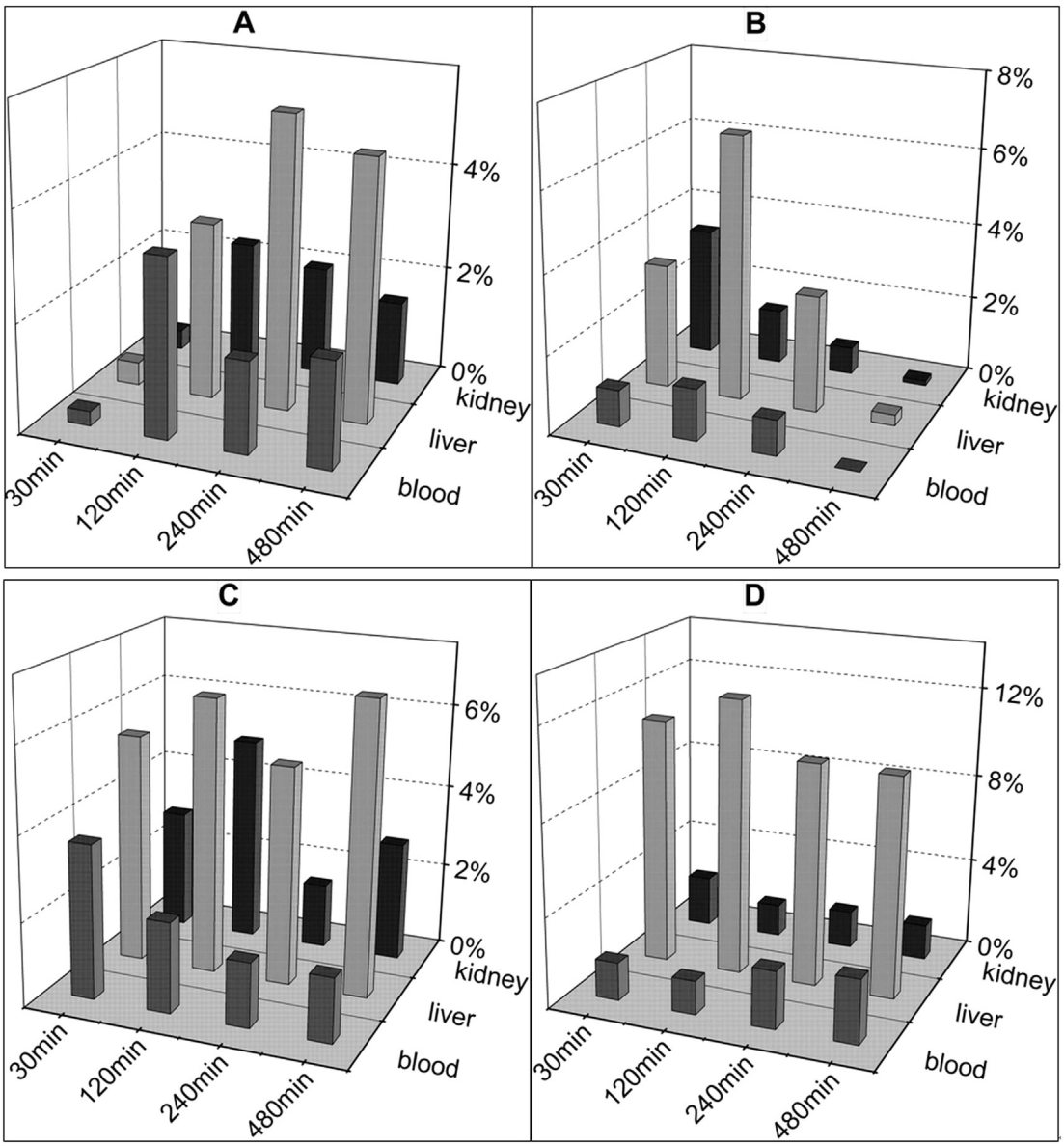

Fig. 6. The changing of tissue distributions of complex **1**(A), **7**(B), **10**(C) and **14**(D) with time.

2.4.1. Metabolism pathways

First, the urine samples from complexes **1**, **7**, **16**–**18** treated rats were inspected with ICP-AES, and found Ru, Cr, Mo and W elements at higher concentration respectively. Second, the urines were concentrated under reduced pressure, and removed partial inorganic salts from the mixtures; the whole process was warm so that the metabolites kept stable. Finally, the gray-like mixtures were obtained and these final mixtures were characterized by IR, XPS and ICP-AES. In the IR spectrum, there is no absorption band in the range of 1800–2100 cm^{-1}; it shows that all metabolites of the complexes do not contain CO ligand. However, some complexes like *fac*-[$M(CO)_3L$] (M = Tc, Re), which used as radiopharmaceuticals for diagnostic and therapy procedures, did not release CO and were excreted essentially in their intact form [57]. Therefore, CO releasing ability is connected with metal properties.

Now that none of CO ligand exists in the structures of metabolites, how did CO ligand in CORMs release during the process of metabolism? Did all CO ligands in complex release completely in liver? In order to further understand the metabolic process, the signals of CO ligand contained in complex **1** were traced through the IR spectra of intermediates. The results showed after treated with liver homogenate, the CO signals of metabolites were strong at the beginning, and then gradually became weak and the absorption bands decreased. And in the IR spectra of metabolites in urine, (Fig. 8, others seen SI-Fig. 5) there was no any signal at 1980–2100 cm^{-1}, so we infer that the loss of CO from the molecule occurred in liver.

As for the fate of the CO ligand liberating in the process of metabolism, there is a possibility to convert to CO_2, because when *fac*-[$Ru(CO)_3Cl(NH_2CH_2COO)$] was incubated with bovine serum albumin, CO_2 but not CO was detected by GC/TCD [50]. This condition is similar to the micro-surrounding of liver cell. The metabolism pathways of CORMs were summed up in Fig. 9.

Carbon monoxide binds as ligand to most transition metals in low oxidation states, like Ru^{II}, W^0. Consequently, most organometallic carbonyl complexes are sensitive to oxidation by oxygen. In XPS spectra of urine metabolites from complexes **1** and **7**, the main peaks observed in the survey scans of different samples are C 1s, Ru

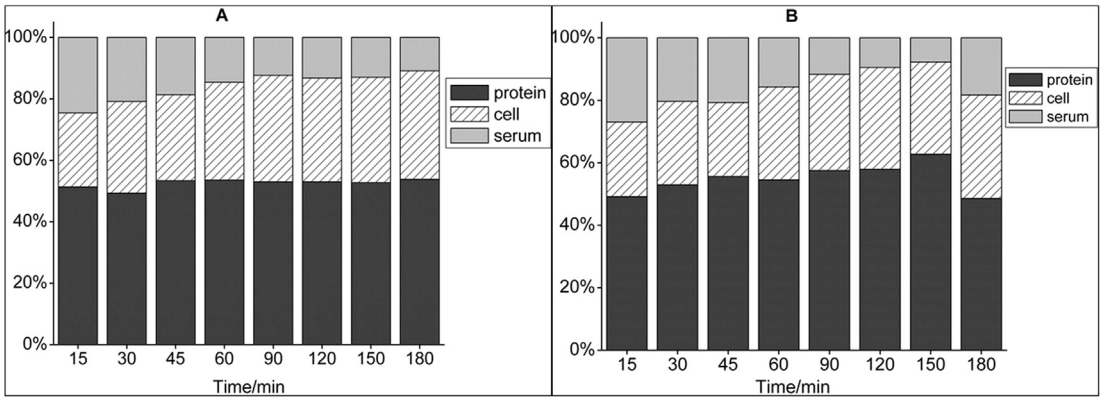

Fig. 7. *In vitro* distribution of complex **1**(A) and **2**(B) in rat whole blood.

3d and 3p, and O 1s peaks, centered at 285, 280–284, 460–480 and 530 eV respectively (Fig. 10). The Ru $3d_{5/2}$ binding energy of complex **1** (285.05 eV) is almost the same as that found for $[Ru^{III}(acac)_3]$ [58]. The binding energy of Ru $3d_{5/2}$ for complex **7** is 285.02 eV. The Ru $3p_{1/2}$ binding energies of complexes **1** and **7** are about 264.05 eV. Such a binding energy value is an indication of the presence of Ru^{III}. As for urine metabolites from complex **17**, the Mo^{IV} $3d_{3/2}$ binding energy is 232.74 eV, Mo^0 $3d_{5/2}$ 228.12 eV, and both of them account for 76.12% and 23.88% respectively. For urine metabolites of complex **18**, the W^{IV} $4f_{7/2}$ binding energy is 33.28 eV, W^0 $4f_{7/2}$ 30.42 eV, and both of them account for 24.60% and 75.40% respectively. Therefore, we infer that Ru^{II} in carbonyl metal complexes was oxidized to Ru^{III} by P450 enzymes, and Ru^{III} is the main form of metabolites. But as for Mo^0 and W^0 in carbonyl metal complexes, part of them transformed into higher oxidation state, the others kept original state.

3. Conclusions

Two series of carbonyl metal CORMs have been preliminarily evaluated through their pharmacokinetic and metabolic processes; the results showed these complexes have drug-like properties. The toxic effects of these complexes were showed by IC_{50} and LD_{50} values. IC_{50} of complex **1** is 62.69 mg/l, complex **7** is 240.16 mg/l, showing a lower cytotoxicity than complex **1**. IC_{50} values of complexes **3**, **4** and **5** are 5–6 times as high as that of complex **1**, and IC_{50} of complex **9** is lower than that. As for those containing Cr and W atom, they showed a stronger toxicity, and IC_{50} values of complexes **16**, **18** are 21.36 mg/l and 22.21 mg/l respectively. *In vivo* toxic experimental data showed LD_{50} values of both complexes **1** and **8** are 800–1000 mg/kg, **7** and **14** 1100–1500 mg/kg; LD_{50} value of complex **10** is only in the range of 150–200 mg/kg. In the case of complexes **16**–**18**, their LD_{50} values are 150–200 mg/kg, 300–500 mg/kg and 75–125 mg/kg respectively. These are in accordance with the results from that of cytotoxicity.

Moreover, these complexes were not found accumulating in main tissues and organs. For example, after i.v. administered 10 min, the amount of complex **1** in blood accounts for 11.46%, and in liver 2.89%, in kidney 6.85%, in lung 2.25%, in heart 0.95% and less than 0.5% in spleen and brain; And 60 min later, it accounts for 7.54% in blood, 2.23% in liver, 4.16% in kidney, 1.45% in lung, 0.46% in heart and less than 0.25% in spleen and brain; blood, liver and

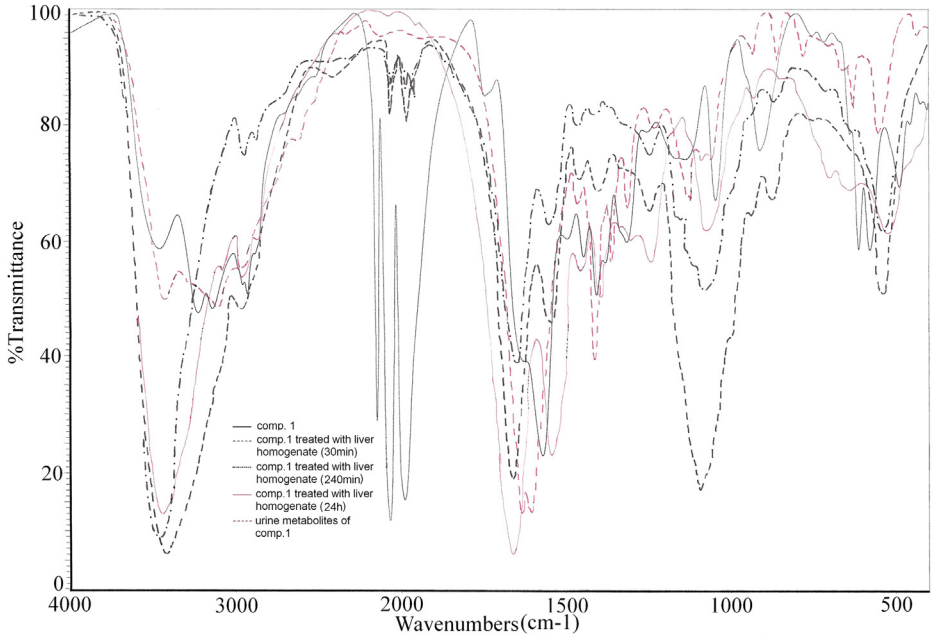

Fig. 8. The changing of IR spectra of complex **1** during the metabolism.

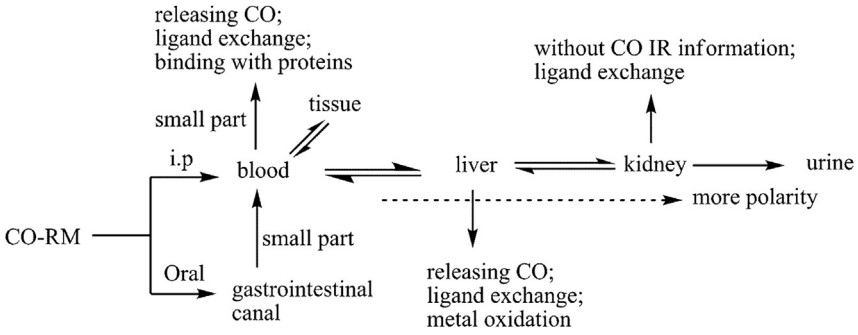

Fig. 9. Metabolism pathways of carbonyl metal CO-releasing molecules.

kidney are main tissues and organs which gathering it. The properties of carbonyl metal CO-releasing molecules determine their rates and extents of absorption and distribution. Complex **8** is insoluble in water, its concentration in liver has arrived at a higher level after 30 min i.p. administered, and accounts for 8.01%; and in 90 min later, the amount in blood, liver and kidney was 4.12%, 4.96% and 4.64% respectively. Compared with complex **1**, more amounts of complex **8** enter lung and spleen at the same time point, but both of them can not enter brain.

Through metabolic process of complexes tracing by FT-IR, and metabolites analyzing by ICP-AES, XPS, we preliminarily proposed the possible metabolism pathway. In the process of metabolism, Ru^{II} in CORMs was oxidized to Ru^{III} by P450 enzymes, and Ru^{III} is the main form of metabolites. But as for Mo^0 and W^0 in carbonyl metal CORMs, part of them transformed into higher oxidation state, the others kept original state.

In the view of IC_{50} of cell toxicity, LD_{50} of toxicity *in vivo* and toxicity to liver and kidney, we infer that complexes **1**–**15** have value in medicine, especially complex **1**. However, we must see the use of these CORMs as medicine is facing many problems, such as confirming the structures of metabolites; however, the biggest one is how to set up a quality standard, because each of them like complexes **1** and **2** will be absorbed in blood, over 50% bound with plasma proteins, and every CORMs has several forms in blood due to hydrolysis. Therefore, to set a quality standard and develop a suitable pharmaceutical form are crucial for next step work.

4. Experimental

4.1. Reagents and instruments

Myoglobin (AR, Sigma), 2.5% glutaraldehyde, 1,2-propylene glycol (AR), deionized water, DMSO (AR), nitric acid (GR), 30% hydrogen peroxide (AR), sodium heparin (AR), $RuCl_3 \cdot xH_2O$ (Ru 38–40%), $Mo(CO)_6$ (AR, Sigma), $Cr(CO)_6$ (AR, Sigma), $W(CO)_6$ (AR, Sigma). All reactions were carried under nitrogen atmosphere. Solvents for reactions were degassed and distilled from the proper drying agents. Column chromatography was carried out using 100–200 mesh silica gel and Al_2O_3.

IR spectra were recorded on a Nicolet NEXUS 360 spectrophotometer, NMR spectra on a Bruker AM-400 MHz spectrometer and elemental analysis (C,H,N) was performed on a Elemental Analyzer vario EL Cube; Beckman-COULTER LX-20 full-auto biochemical analyzer; JEM-1230 transmission electron microscope; Lambda 25 UV–visible spectrophotometer; Maxis-4G TOF Mass spectrometer; IRIS-Advantage-ER/S ICP-AES (spectral line for measurement, Ru 267.876 nm, Cr 267.716 nm, Mo 202.030 nm, W 239.709 nm).

4.2. CO release tests with a myoglobin assay

The release of CO from the metal carbonyl complexes was studied spectrophotometrically by measuring the conversion of deoxy-myoglobin (deoxy-Mb) to carbonyl myoglobin (CO-Mb). The

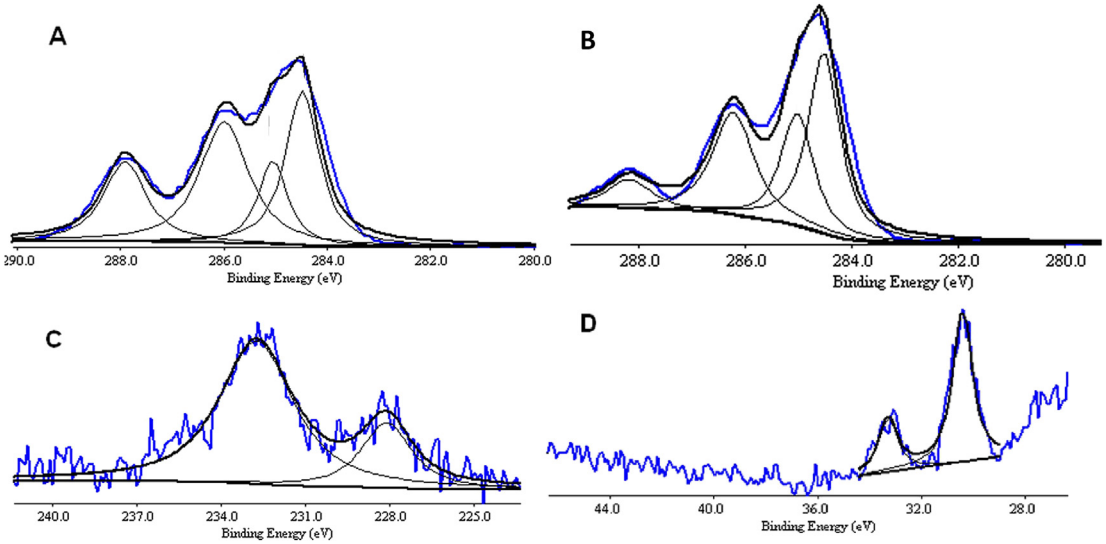

Fig. 10. X-ray photoelectron spectroscopies of urine metabolites, A for complex **1** and B for complex **7**, C for **17**, D for **18**.

amount of CO-Mb formed was quantified by measuring the absorbance at 540 nm. A stock solution of myoglobin (60 μM final concentration) was prepared fresh by dissolving the protein in PBS (0.1 M, pH = 7.4). Sodium dithionite (0.1%) was added to convert the myoglobin to deoxy-Mb. A 2 ml quantity of this was measured to obtain a deoxy-Mb spectrum and then bubbled with CO to get a CO-Mb spectrum. Complexes were dissolved in an appropriate solvent (DMSO or MeOH) and added to deoxy-Mb in the cuvette (to give a final complex concentration of 20, 40, 60 μM), mixed using a pipette and then overlaid with 500 μl light mineral oil to prevent CO escaping or the myoglobin being oxygenated.

The maximal absorption peak of deoxy-Mb at 560 nm is converted to the two maximal absorption peaks of CO-Mb at 540 and 578 nm. CO-releasing half-lives of complexes were determined according to the literature method [53] and the absorbance at 510 nm, 540 nm was used.

4.3. Lipophilicity (log P o/w)

The lipophilicity of complexes was determined using the flask-shaking method where *n*-octanol and 0.1 M PBS were used as the organic and aqueous phase respectively. *n*-Octanol was pre-saturated with 0.1 M PBS by swirling at 45 rpm for 24 h. The tested complex was dissolved in the isolated organic phase at a concentration of 50 μM. An equal volume of aqueous PBS was added, and the mixture was swirled for 8 h at 45 rpm at 37 °C. The solution was then centrifuged, and the amounts of complex in both layers were determined by ICP-AES.

4.4. Cytotoxic assay

The L929 murine fibroblast cells line was purchased from Cell Resources Center for Shanghai Life Science Institute of Chinese Academy of Sciences (China). The cells were cultivated at 37 °C, 10% CO_2, 100% humidity in RPMI1640 medium, enriched with glucose and supplemented with 10% fetal bovine serum, non-essential amino acids, antibiotics (penicillin/streptomycin) and antifungals.

Typically, 0.126 mmol of complex was dissolved in 0.6 ml of DMSO, which after homogenization was injected over 10 ml of culture medium with vigorous stirring at 55 °C. Growth inhibitory effect toward fibroblast cell line was determined by means of MTT colorimetric assay. The cells were seeded into 96-well plates at 6×10^3 cells/well and a certain volume of the above solution was added. Culture medium was added until completion of 0.2 ml and the final concentration of complexes in each well was 100–1600 μM. Triplicate cultures were established for all complexes and for the control. The mixture was incubated at 37 °C in a humid atmosphere containing 10% CO_2 for 24 h. Cell viability was quantified after 24 h by the MTT method.

4.5. Protocol and animal treatment

All animal (male Wistar rat and male Kunming mouse) procedures were approved by the institutional ethics committee. All mice and rats were maintained in cages with a 12 h light/dark cycle and free access to standard diet and water. Mice and rats were housed and cared for by the veterinary staff in accredited facilities and were routinely screened for health status. The mice and rats used were between 10 and 12 weeks of age.

4.6. Toxicity in vivo and LD_{50}

The oral acute toxic class method (ATC method) was used to measure the oral LD_{50} of complexes. Complexes were dissolved in distilled water or suspended in 0.4% CMC-Na solutions before each experiment. And those solutions or suspensions were administered through oral with a volume of 0.4 ml and gradient doses of 2000 mg/kg, 300 mg/kg, 50 mg/kg and 5 mg/kg. Three male mice (20 ± 1 g) were used for per dose group of each complex, and during the experimental process, the experimental details and results were done according to literature method [55].

4.7. Distribution of the complexes in tissues and organs

Kunming mouse (25 ± 1 g) was used and complexes were administered i.p. or i.v. at 0.1–0.25 mmol/kg (for Ru^{II} contained complexes, 0.25 mmol/kg, and for group 6 metal contained complexes, 0.1 mmol/kg). Complexes were freshly prepared before each experiment by dissolving complexes in DMSO–H_2O (20–80%) mixture solvent or other proper solvents. And then the animals were sacrificed by amputating head after 30 min, 120 min, 240 min and 480 min respectively, their bloods were collected and anti-coagulated with sodium heparin; their intact organs were separated and washed with distilled water and ethanol. Then all the tissues and organs were digested with 3 ml concentrated nitric acid and 1 ml H_2O_2 at 90 °C for 8 h. The digested solutions were reconstituted to 5 ml with distilled water and ICP-AES was used to analyze their metal ion concentrations. Finally, the accurate metal ions amounts of each tissue and organ were converted into the data of their percentage contents compared with the total amounts of metal ions administered.

4.8. Distribution of complexes in whole blood

0.05 mmol complex **1** was dissolved in 100 μl normal saline, and then 80 μl solution was added into 4 ml fresh rat anticoagulant whole blood; the whole blood was mixed and incubated in dark at 37 °C. In the time points of 15 min, 30 min, 45 min, 60 min, 90 min, 120 min, 150 min and 180 min respectively, 400 μl whole blood was extracted in each time point and treated according to procedure in SI-Fig. 4. Then every part of the whole blood was digested and ruthenium contents in blood cells, serum and proteins were measured using ICP-AES.

Distribution of complex **2** in whole blood was analyzed with the same procedure for complex **1**.

4.9. Metabolism of the complexes

Using Wistar rats: Complexes were administered i.p. at 0.05–0.125 mmol/kg per day for 8–21 days (SI-Table 5). These doses were selected due to their activity and toxicity. Complexes were freshly prepared before each experiment by dissolving them in 1 ml 10% propylene glycol or distilled water. The same volume of solvent was injected in the control group. During the experimental process, fresh urine samples were collected per 12 h with metabolism cages and stored in 4–8 °C. After 8–21 days later, animals were fasted 12 h, and then sacrificed by amputating head and the blood samples were obtained, part of their liver and kidney were separated and treated with 2.5% glutaraldehyde for histological analysis.

The fresh blood samples were evaluated through blood biochemical analysis. The urine samples treated with 0.45 μm filter membrane were analyzed by ICP-AES and urine routine examination; after concentrated under reduced pressure and removed partial inorganic salts using methanol, the urine samples gave gray white powders, and these powders were analyzed by FIT-IR, XPS and ICP-AES.

The metabolism of complex in liver homogenate was carried as following: Comp. **1** 100 mg was dissolved in 1 ml distilled water and

then added into 10 ml 20% mouse liver homogenate freshly prepared in distilled water, this mixture was incubated at 37 °C (dark, N_2 atmosphere). In every certain time point, 1.5 ml mixture was extracted and centrifuged to get the supernatant solution. After evaporated solvents under reduced pressure and warm condition, the residue of the supernatant solution was measured by FT-IR to show the metabolism of metal CO with time. The sample of comp. **1** without treatment was gotten through evaporating its fresh distilled water solution under the same condition, and the spectrum of urine metabolites of comp. **1** was gotten from the former step of this section.

4.10. Syntheses

4.10.1. Preparation of 2-amino-6-(2-hydroxybenzamido) hexanoic acid (*L*$_1$)

A solution of 1.232 g of $CuSO_4 \cdot 5H_2O$ in 10 ml distilled water was added to aqueous solution of 1.5 g L-lysine hydrochloride. The mixture refluxed at 80 °C for 2 h, and got a mazarine solution. The solvent was removed under reduced pressure to get raw blue solid. With methanol and acetone washing, blue solid 1.402 g was obtained with 80.0% yield.

The blue solid above dissolved in 15 ml distilled water, adjusted its pH to 8.5–9.0 with 2 M sodium hydroxide, and then added a solution of active ester prepared from salicylic acid and N-hydroxysuccinimide to the former solution under ice-bath condition. In 1 h later, the ice-bath drew back and the mixture was overnight with stirring at room temperature. Part solvent was removed under reduced pressure, and dust blue precipitate appeared. The precipitate was washed with distilled water, methanol and ether respectively, and a 1.17 g portion of pale blue powder was obtained after dryness at room temperature. Then, the blue powder was suspended into distilled water, following adding aqueous solution of sodium sulfide to suspended solution; the mixture was stirred for 10 min at room temperature, and the black precipitate was filtered off. The filtrate was treated with active charcoal until the solution became colorless. After adjusting pH to 6.0 ~ 7.0 with 10% hydrochloric acid, the white solid started to appear. Collecting white solid, it weighed 0.7954 g and the total yield was 48.2%. m.p. 179–181 °C; IR (KBr, cm^{-1}): 3407.4 (s, Ar–OH), 2938.5 (m, NH_2), 1709.7 (w, *C*OOH), 1637.8 (m, *C*ONH), 1586.9 (v, Ar–*C*=*C*), 1550.9 (m, CO*NH*), 747 (m, Ar–*CH*). ^{1}H NMR (DMSO-d_6: D_2O = 1:1, TMS, ppm): δ 7.669 (d, 1H, J = 7.6 Hz, Ar–H_6), 7.136 (m, 1H, Ar–H_4), 6.598 (d, 1H, J = 8.0 Hz, Ar–H_3), 6.455 (t, 1H, J = 7.2 Hz, Ar–H_5), 3.773 (dd, 1H, J_1 = 5.6 Hz, J_2 = 6.8 Hz, α-CH), 3.274 (d, 2H, J = 6.8 Hz, ε-CH_2), 1.597 (m, 2H, β-CH_2), 1.536 (m, 2H, δ-CH_2), 1.500 (m, 2H, γ-CH_2). ESI-MS: calcd for $C_{13}H_{19}N_2O_4$ $[M+H]^+$ 267.1345, found 267.1354. Elemental Anal. Calcd for $C_{13}H_{18}N_2O_4$: C, 58.63; H, 6.81; N, 10.52%. Found: C, 58.71; H, 6.96; N, 10.46%.

4.10.2. Preparation of L-cysteine methyl ester hydrochloride (*L*$_2$)

Under ice-bath condition, 3 ml $SOCl_2$ was added dropwise to 35 ml methanol in the presence of nitrogen atmosphere. Afterward, the solution was stirred at room temperature for 1 h, then 1 g $Cys \cdot HCl \cdot H_2O$ was added in batches to the solution. And the mixture solution reacted at room temperature for 3 h, and then refluxed for 1 h. Removing the volatile component and solvent, the residue was recrystallized with CH_3OH–CH_2Cl_2, and 0.84 g white solid was obtained with 85.9% yield. IR (KBr, cm^{-1}): 3040.4 (s, NH_2), 1709.7 (s, C=O), 2580 (w, SH). ^{1}H NMR (D_2O, TMS, ppm); δ 4.453 (t, 1H, CH, J = 5.2 Hz), 3.871 (s, 3H, CH_3), 3.164 (t, 2H, CH_2, J = 6.4 Hz). Elemental Anal. Calcd for $C_4H_{10}NO_2SCl$: C, 27.99; H, 5.87; N, 8.16%. Found: C, 28.11; H, 6.01; N, 8.08%.

4.10.3. Preparation of 2-(pyridin-2-yl-carbamoyl) phenyl acetate (*L*$_3$)

A solution of 5 mmol of 2-acetyloxy-benzoyl chloride in THF was added dropwise to the solution of 460 mg of 2-amino pyridine and 1 ml of triethylamine in THF under ice-bath condition. After that, the mixture was stirred for 3 h at room temperature. Then the white precipitate was removed and the filtrate was concentrated. The residue was purified through gel column chromatography using methanol–chloroform as eluent. 0.401 g pale yellow solid obtained with 32.1% yield. IR (KBr, cm^{-1}): 1730.7 (s, CH_3*C*OO), 1677.8 (s, *C*ONH), 1586.9 (s, Ar–*C*=*C*), 1570.2 (m, CO*NH*), 745 (m, Ar–*CH*). ^{1}H NMR (DMSO-d_6, TMS, ppm) δ: 11.742 (br, 1H, NH), 8.321 (m, 1H, pyridine ring-H_6), 8.241 (d, 1H, J = 8.0 Hz, pyridine ring-H_3), 7.921 (d, 1H, J = 8.0 Hz, Ar–H_6), 7.253–7.485 (m, 4H, 3H in Ar and 1H in pyridine ring-H_4), 6.652 (m, 1H, pyridine ring-H_5), 2.080 (s, 3H, $COCH_3$). ESI-MS: calcd for $C_{14}H_{13}N_2O_3$ $[M+H]^+$ 257.0926, found 257.0972. Elemental Anal. Calcd for $C_{14}H_{12}N_2O_3$: C, 65.62; H, 4.72; N, 10.93%. Found: C, 66.01; H, 4.91; N, 10.98%.

4.10.4. Preparation of 2-(pyridin-3-yl-carbamoyl) phenyl acetate (*L*$_4$)

The reaction procedure and workup were the same as those of **L$_3$**. A 0.470 g portion of pale yellow solid was isolated with yield 37.5%. IR (KBr, cm^{-1}): 1734.2 (s, CH_3*C*O), 1689.1 (s, *C*ONH), 1584.1 (m, Ar–*C*=*C*), 1568.5 (m, CO*NH*), 747 (m, Ar–*CH*). ^{1}H NMR (DMSO-d_6, TMS, ppm) δ: 10.644 (br, 1H, NH), 8.865 (d, 1H, J = 6.4 Hz, pyridine ring-H_2), 8.294 (d, 1H, J = 5.2 Hz, pyridine ring-H_6), 8.109 (m, 1H, pyridine ring-H_4), 7.925 (dd, 1H, J_1 = 1.6 Hz, J_2 = 8.0 Hz, Ar–H_6), 7.436 (m, 2H, Ar–H_4, pyridine ring-H_5), 7.029 (m, 2H, Ar–$H_{3,5}$), 2.081 (s, 3H, $COCH_3$). ESI-MS: calcd for $C_{14}H_{13}N_2O_3$ $[M+H]^+$ 257.0926, found 257.0942. Elemental Anal. Calcd for $C_{14}H_{12}N_2O_3$: C, 65.62; H, 4.72; N, 10.93%. Found: C, 65.83; H, 5.01; N, 11.06%.

4.10.5. Preparation of 2-(pyridin-4-yl-carbamoyl) phenyl acetate (*L*$_5$)

The reaction procedure and workup were the same as those of **L$_3$**. A 1.0574 g portion of yellow solid was isolated with yield 28.3%. IR (KBr, cm^{-1}): 1740.1 (s, CH_3*C*O), 1654.2 (s, *C*ONH), 1581.9 (m, Ar–*C*=*C*), 1581.2 (m, CO*NH*), 741 (m, Ar–*CH*). ^{1}H NMR (DMSO-d_6, TMS, ppm) δ: 10.532 (br, 1H, CONH), 8.444 (m, 2H, pyridine ring-$H_{2,6}$), 7.864 (dd, 1H, J_1 = 1.6 Hz, J_2 = 8.0 Hz, Ar–H_6), 7.741 (m, 2H, pyridine ring-$H_{3,5}$), 7.435 (m, 1H, Ar–H_4), 7.013 (m, 2H, Ar–$H_{3,5}$), 2.086 (s, 3H, $COCH_3$). ESI-MS: calcd for $C_{14}H_{13}N_2O_3$ $[M+H]^+$ 257.0926, found 257.0961. Elemental Anal. Calcd for $C_{14}H_{12}N_2O_3$: C, 65.62; H, 4.72; N, 10.93%. Found: C, 65.93; H, 4.86; N, 10.82%.

4.10.6. Preparation of 2-((pyridin-2-ylmethyl)-carbamoyl) phenyl acetate (*L*$_6$)

The reaction procedure and workup were the same as those of **L$_3$**. A 0.942 g portion of pale yellow oil was isolated with yield 51.2%. IR (KBr, cm^{-1}): 1738.1 (s, CH_3*C*O), 1657.1 (s, *C*ONH), 1585.4 (m, Ar–*C*=*C*), 1583.7 (m, CO*NH*), 744 (m, Ar–*CH*). ^{1}H NMR (DMSO-d_6, TMS, ppm) δ: 9.472 (br, 1H, NH), 8.642 (m, 1H, pyridine ring-H_6), 7.927 (dd, 1H, J_1 = 1.2 Hz, J_2 = 8.0 Hz, Ar–H_6), 7.823 (m, 1H, pyridine ring-H_4), 7.252–7.583 (m, 5H, 2H in pyridine and 3H in Ar), 4.693 (d, 2H, J = 5.6 Hz, NCH_2), 2.081 (s, 3H, $COCH_3$). ESI-MS: calcd for $C_{15}H_{15}N_2O_3$ $[M+H]^+$ 271.1083, found 271.1068. Elemental Anal. Calcd for $C_{15}H_{14}N_2O_3$: C, 66.66; H, 5.22; N, 10.36%. Found: C, 66.97; H, 5.46; N, 10.19%.

4.10.7. Preparation of ligand *L*$_7$ and *L*$_8$

L$_7$ Salicylidene ethylenediamine Schiff base: The solution of 0.56 ml of salicylaldehyde in 10 ml ethanol was added dropwisely to the solution of 0.4 ml ethylenediamine and 2–3 drops acetic acid in 15 ml ethanol under ice-bath condition. The mixture was stirred

for 1 h, then drew back ice-bath and continued to react for 3 h at room temperature. The major solvent was removed under reduced pressure. The solution was cooled and yellow solid was obtained. After recrystallization, 603.5 mg yellow crystal was obtained with yield 68.2%. IR (KBr, cm^{-1}): 3429.4 (s, Ar–OH), 1572.5 (s, Ar–*C*=*C*), 748 (m, Ar–*CH*). ^1H NMR (DMSO-d_6, TMS, ppm) δ: 11.264 (br, 1H, OH), 8.513 (s, 1H, CH=N), 7.452 (d, 1H, Ar–H_6), 7.124 (m, 1H, Ar–H_4), 6.852 (m, 1H, Ar–H_5), 6.761 (d, 1H, Ar–H_3), 4.126 (br, 2H, NH_2), 3.812 (t, 2H, CH=NCH_2), 3.012 (t, 2H, NH_2CH_2). Elemental Anal. Calcd for $C_9H_{12}N_2O$: C, 65.83; H, 7.37; N, 17.06%. Found: C, 65.70; H, 7.46; N, 17.18%.

L_8 Salicylidene 2-amino-pyridine Schiff base: The procedure and work-up were the same as that of **L_7**. 761.3 mg orange crystal was obtained with yield 71.1%. IR (KBr, cm^{-1}): 3427.2 (s, Ar–OH), 1576.1 (s, Ar–*C*=*C*), 740 (m, Ar–*CH*). ^1H NMR (DMSO-d_6, TMS, ppm) δ: 12.251 (br, 1H, OH), 9.207 (s, 1H, CH=N), 8.640 (d, 1H, pyridine H_6), 7.821 (m, 1H, pyridine H_3), 7.112–7.413 (m, 4H, 2H in Ar and 2H in pyridine), 6.811–6.813 (m, 2H, Ar–$H_{3,5}$). Elemental Anal. Calcd for $C_{12}H_{10}N_2O$: C, 72.71; H, 5.08; N, 14.13%. Found: C, 72.80; H, 5.17; N, 14.02%.

4.10.8. Preparation of $[Ru(CO)_3Cl_2]_2$

In the presence of nitrogen atmosphere, 2 g $RuCl_3 \cdot xH_2O$ was added to the solution of 25 ml of formic acid and 12.5 ml of concentration hydrochloric acid. The mixture was refluxed at 110 °C until the solution became from deep red to pale yellow. The solvent was removed under reduced pressure. The residue was recrystallized with CH_2Cl_2–*n*-pentane, and milk-white powder 1.6 g was obtained, the yield was 85%. IR (KBr, cm^{-1}): 2139.5 (s, CO), 2088.7 (s, CO), 2071.8 (s, CO), 2057.2 (s, CO).

4.10.9. Preparation of $Ru(CO)_3Cl$-glycinate (**1**) [59]

$[Ru(CO)_3Cl_2]_2$ (147.8 mg,0.29 mmol) and glycine (43.5 mg, 0.58 mmol) were placed under nitrogen in a round-bottomed flask. Methanol (15 ml) and sodium methoxide (32 mg, 0.59 mmol) were added and the reaction was allowed to continue under stirring for 24 h at room temperature. The solvent was then removed under pressure and the yellow residue redissolved in tetrahydrofuran (THF); this was filtered and excess light petroleum added. The yellow solution was evaporated down to give a pale yellow solid (153.9 mg, 90.1% yield). It was stored in closed vials at −20 °C and used freshly on the day of the experiments. IR (KBr, cm^{-1}): 3223.3 (m, NH_2), 3137.7 (m, NH_2), 2143.5 (s, CO), 2065.0 (s, CO), 1989.0 (s, CO), 1569.8 (s, COO^-). ^1H NMR (DMSO-d_6, TMS, ppm): δ 5.398 (br, 1H, NH), 4.723 (br, 1H, NH), 3.479 (m, 1H, CH), 3.249 (m, 1H, CH). ^{13}C NMR (DMSO-d_6, TMS, ppm): δ 200.9 (Ru–CO), 198.5 (Ru–CO), 196.9 (Ru–CO), 181.1, 180.7, 41.3. ESI-MS: calcd for $C_5H_4NO_5ClRuNa$ $[M+Na]^+$ 317.8719, found 317.8611. Elemental Anal. Calcd for $C_5H_4NO_5ClRu$: C, 20.38; H, 1.37; N, 4.75%. Found: C, 20.94; H, 1.68; N, 4.27%.

Complexes **2**–**5** [60] were synthesized following the same procedure as for complex **1**, but changing amino acid or other ligand.

4.10.10. Preparation of $Ru(CO)_3Cl$-alaninate (**2**)

A 424.3 mg portion of pale yellow solid was isolated with yield 89.3%. IR (KBr, cm^{-1}): 3234.6 (w, $-NH_2$), 3146.9 (w, NH_2), 2141.1 (m, CO), 2062.3 (s, CO), 1986.2 (s, CO), 1619.74 (s, *COO*). ^1H NMR (DMSO-d_6, TMS, ppm): δ 5.652 (br, 1H, NH), 5.436 (br, 1H, NH), 3.465 (q, 1H, $J = 6.8$ Hz, CH), 1.259 (d, 3H, $J = 7.2$ Hz, CH_3). ^{13}C NMR (DMSO-d_6, TMS, ppm): δ 200.0 (Ru–CO), 198.6 (Ru–CO), 197.1 (Ru–CO), 183.1, 50.6, 18.3. ESI-MS: calcd for $C_6H_6NO_5ClRuNa$ $[M+Na]^+$ 331.8876, found 331.8736. Elemental Anal. Calcd for $C_6H_6NO_5ClRu$: C, 23.35; H, 1.96; N, 4.54%. Found: C, 24.55; H, 2.59; N, 4.28%.

4.10.11. Preparation of $Ru(CO)_3Cl$-L-valinate (**3**)

A 440.8 mg portion of yellow solid was isolated with yield 90.7%. IR (KBr, cm^{-1}): 3232.8 (w, NH_2), 3135.9 (w, NH_2), 2966.2 (m, CH), 2140.6 (s, CO), 2061.9 (v, CO), 1986.9 (v, CO), 1628.1 (s, *COO*). ^1H NMR (DMSO-d_6, TMS, ppm): δ 6.187 (br, 1H, NH), 5.684 (br, 1H, NH), 3.827 (d, 1H, α-CH), 2.175 (m, 1H, β-CH), 0.972 (d, $J = 5.6$ Hz, CH_3), 0.954 (d, $J = 5.6$ Hz, CH_3). ^{13}C NMR (DMSO-d_6, TMS, ppm): δ 201.1 (Ru–CO), 197.9 (Ru–CO), 197.3 (Ru–CO), 181.8, 59.6, 30.9, 18.8, 18.4. ESI-MS: calcd for $C_8H_{10}NO_5ClRuNa$ $[M+Na]^+$ 359.9189, found 359.9048. Elemental Anal. Calcd for $C_8H_{10}NO_5ClRu$: C, 28.54; H, 2.99; N, 4.16%. Found: C, 28.30, H, 3.68; N, 3.71%.

4.10.12. Preparation of $Ru(CO)_3Cl$-D-valinate (**4**)

A 420.3 mg portion of yellow solid was isolated with yield 94.8%. IR (KBr, cm^{-1}): 3233.3 (w, NH_2), 3132.9 (w, NH_2), 2965.9 (m, CH), 2141.0 (s, CO), 2061.7 (v, CO), 1985.6 (v, CO), 1632.7 (s, *COO*), 1564.0 (m, NH_2). ^1H NMR (DMSO-d_6, TMS, ppm): δ 6.186 (br, 1H, NH), 5.682 (br, 1H, NH), 3.828 (d, 1H, α-CH), 2.173 (m, 1H, β-CH), 0.986 (d, $J = 5.6$, CH_3), 0.956 (d, $J = 6.4$ Hz, CH_3). ^{13}C NMR (DMSO-d_6, TMS, ppm): δ 201.0 (Ru–CO), 197.9 (Ru–CO), 197.5 (Ru–CO), 181.6, 180.9, 59.6, 30.7, 18.8, 18.4. ESI-MS: calcd for $C_8H_{10}NO_5ClRuNa$ $[M+Na]^+$ 359.9189, found 359.9036. Elemental Anal. Calcd for $C_8H_{10}NO_5ClRu$: C, 28.54, H, 2.99; N, 4.16%. Found: C, 28.25, H, 3.46; N, 3.79%.

4.10.13. Preparation of $Ru(CO)_3Cl$-L-phenylalaninate (**5**)

A 524.9 mg portion of yellow solid was isolated with yield 93.9%. IR (KBr, cm^{-1}): 3134.0 (w, NH_2), 2139.8 (s, CO), 2062.4 (v, CO), 1987.3 (v, CO), 1631.1 (s, *COO*), 1572.4 (m, Ar C=C). ^1H NMR (DMSO-d_6, TMS, ppm): δ 7.445–7.220 (m, 5H, Ar–H), 6.163 (br, 1H, NH), 5.745 (br, 1H, NH), 3.845 (d, 1H, $J = 7.6$ Hz, α-CH,), 2.976 (m, 1H, β-CH), 2.816 (m, 1H, β-CH). ^{13}C NMR (DMSO-d_6, TMS, ppm): δ 201.6 (Ru–CO), 197.9 (Ru–CO), 196.0 (Ru–CO), 182.3, 138.9, 139.3, 127.1, 126.6, 55.7, 37.6. ESI-MS: calcd for $C_{12}H_{10}NO_5ClRuNa$ $[M+Na]^+$ 407.9189, found 407.9047. Elemental Anal. Calcd for $C_{12}H_{10}NO_5ClRu$: C, 37.46; H, 2.62; N, 3.64%. Found: C, 37.92; H, 2.98; N, 3.36%.

4.10.14. Preparation of $Ru(CO)_3Cl$-**L_1** (**6**)

The procedure was the same as that of complex **1** except **L_1** taking the place of glycine ligand. 549.1 mg yellow solid powder was obtained with yield 90.3%. IR (KBr, cm^{-1}): 3408.4 (s, Ar–OH), 2938.5 (m, CH), 2128.6 (v, CO), 2057.3 (v, CO), 1989.4 (v, CO), 1630.6 (s, COO), 1586.9 (s, COON), 1550.9 (m, COOH). ^1H NMR (DMSO-d_6, TMS, ppm): δ 12.786 (bs, 1H, Ar–OH), 8.882 (bs, 1H, CONH), 7.886 (d, 1H, $J = 6.8$ Hz, Ar–H_6), 7.391 (t, 1H, $J = 7.6$ Hz, Ar–H_4), 6.859–6.900 (m, 2H, Ar–$H_{3,5}$), 6.385 (br, 1H, NH), 5.882 (br, 1H, NH), 3.425 (t, 1H, α-CH), 3.304 (m, 2H, ε-CH_2), 1.425–1.729 (m, 6H, CH_2). ^{13}C NMR (DMSO-d_6, TMS, ppm): δ 200.0 (Ru–CO), 198.1 (Ru–CO), 197.5 (Ru–CO), 183.9, 181.1, 165.8, 158.5, 133.9, 130.1, 120.4, 118.3, 115.5, 55.8, 39.1, 33.2, 29.7, 23.9. ESI-MS: calcd for $C_{16}H_{17}N_2O_7ClRuNa$ $[M+Na]^+$ 508.9665, found 508.9575. Elemental Anal. Calcd for $C_{16}H_{17}N_2O_7ClRu$: C, 39.55; H, 3.53; N, 5.77%. Found: C, 40.03; H, 3.91; N, 5.52%.

4.10.15. Preparation of $Ru(CO)_3Cl$-**L_2** (**7**)

The procedure was the same as that of complex **1** except **L_2** taking the place of glycine ligand. 365.3 mg orange solid powder was obtained with yield 90.1%. IR (KBr, cm^{-1}): 3200.3 (m, NH_2), 3111.1 (m, NH_2), 2129.0 (s, CO), 2058.3 (s, CO), 1988.4 (s, CO), 1742.3 (s, *COO*). ^1H NMR (DMSO-d_6, TMS, ppm): δ 6.395 (br, 1H, NH), 5.982 (br, 1H, NH), 4.388 (t, 1H, $J = 4.8$ Hz, CH), 3.735 (s, 3H, CH_3), 3.021 (t, 2H, $J = 6.4$ Hz, CH_2). ^{13}C NMR (DMSO-d_6, TMS, ppm): δ 201.9 (Ru–CO), 199.6 (Ru–CO), 198.1 (Ru–CO), 173.5, 53.1, 47.9, 25.8. ESI-MS: calcd for $C_7H_8NO_5ClSRuNa$ $[M+Na]^+$ 377.8753, found 377.8632.

Elemental Anal. Calcd for $C_7H_8NO_5ClSRu$: C, 23.70; H, 2.27; N, 3.95%. Found: C, 24.33; H, 2.75; N, 3.71%.

4.10.16. Preparation of $Ru(CO)_3Cl$-Acac (**8**)

509.5 mg orange solid was obtained after recrystallization in 81.1% yield. IR (KBr, cm^{-1}): 2925.5 (w, CH), 2134.4 (w, CO), 2067.4 (s, CO), 1998.6 (s, CO), 1627.2 (m, C=O), 1523.1 (w, C=C). ^1H NMR (DMSO-d_6, TMS, ppm): δ 5.578 (s, 1H, CH=C), 3.346 (s, 6H, $2CH_3$). ^{13}C NMR ($CDCl_3$, TMS, ppm): δ 197.0 (Ru–CO), 186.8 (Ru–CO), 99.4 (CH_3CO), 46.8 (CH), 28.1 (CH_3). ESI-MS: calcd for $C_8H_7O_5ClRuNa$ $[M+Na]^+$ 342.8923, found 342.8801. Elemental Anal. Calcd for $C_8H_7O_5ClRu$: C, 30.06; H, 2.21%. Found: C, 30.21; H, 2.38%.

4.10.17. Preparation of $[Ru(bpy)(CO)_3Cl]^+$ $[Cl]^-(H_5O_2)^+Cl^-$ (**9**) [61]

$[Ru(CO)_3Cl_2]_2$ (500 mg) and 625 mg of 2,2′-bipyridine were dissolved separately in 5 ml of ethylene glycol. Solutions were gently heated until reagents were completely dissolved. Solutions were combined and stirred for 2 h at room temperature. Pale yellow started to precipitate almost immediately after combining of the solutions. The solid product was washed with 2-propanol and hexane and dried under vacuum. The complex obtained above was dissolved in a little amount of concentrated HCl under air. After a few minutes, nearly colorless solid started to crystallize. The solution was allowed to evaporate to dryness at room temperature. The total yield was 46%. IR (KBr, cm^{-1}): 2112.4 (s, CO), 2060.7 (v, CO), 1993.3 (v, CO), 1602.8 (s, pyridine C=C). ^1H NMR ($CDCl_3$, ppm): δ 9.202 (d, 2H, $J=7.2$ Hz), 8.814 (d, 2H, $J=8.0$ Hz), 8.210 (t, 2H, $J=7.6$ Hz), 7.879 (t, 2H, $J=6.4$ Hz). ^{13}C NMR ($CDCl_3$, ppm): δ 188.1 (Ru–CO), 184.5 (Ru–CO), 157.2, 156.3, 143.5, 130.0, 126.6. Elemental Anal. Calcd for $C_{13}H_{13}N_2O_5Cl_3Ru$: C, 32.21; H, 2.70; N, 5.78%. Found: C, 32.41; H, 2.92; N, 5.63%.

4.10.18. Preparation of $[Ru(CO)_3Cl_2$-**L_3**$]$ (**10**) [56]

$[Ru(CO)_3Cl_2]_2$ (256.1 mg, 0.50 mmol) was added to the solution of 256.0 mg (1.00 mmol) **L_3** in 15 ml of deoxygenated 1,2-dimethoxyethane. Then the solution was heated at 60 °C, and the mixture was stirred for 6 h in the presence of nitrogen atmosphere. After filtering, the solvent was removed under vacuum, the residue was extracted by minimum amount of THF. After removing solvent under vacuum 473.02 mg pale yellow solid was obtained with yield 92.4%. IR (KBr, cm^{-1}): 3079.9 (w, NH), 2134.3 (s, CO), 2065.6 (s, CO), 1955.8 (s, CO), 1765.8 (m, *COO*), 1641.0 (s, *CO*NH), 1615.8 (s, pyridine C=C), 1478.6 (s, Ar C=C). ^1H NMR (DMSO-d_6, TMS, ppm): δ 12.889 (s, 1H, NH), 8.793 (d, 1H, $J=5.6$ Hz, Ar–H), 8.253 (t, 1H, $J=7.6$ Hz, Ar–H), 7.863 (d, 1H, $J=6.8$ Hz, Ar–H), 7.772 (t, 1H, $J=7.2$ Hz, Ar–H), 7.642 (d, 1H, $J=8.4$ Hz, Ar–H), 7.588 (t, 1H, $J=6.4$ Hz, Ar–H), 7.523 (t, 1H, $J=7.2$ Hz, Ar–H), 7.413 (d, 1H, $J=7.6$ Hz, Ar–H), 2.331 (s, 3H, CH_3). ^{13}C NMR (DMSO-d_6, TMS, ppm): δ 196.6 (Ru–CO), 195.1 (Ru–CO), 168.8 (*CO*N, *COO*), 148.7, 148.1, 142.2, 134.1, 130.0, 126.0, 125.8, 124.2, 122.9, 117.9, 20.9. ESI-MS: calcd for $C_{17}H_{13}O_6Cl_2N_2Ru$ $[M+H]^+$ 512.9194, found 512.9097. Elemental Anal. Calcd for $C_{17}H_{12}N_2O_6Cl_2Ru$: C, 39.86; H, 2.36; N, 5.47%. Found: C, 40.26; H, 2.72; N, 5.62%.

4.10.19. Preparation of $[Ru(CO)_3Cl_2$-**L_4**$]$ (**11**)

Complexes **11**–**13** were synthesized following the same procedure as for complexes **10**, but changing the ligand from **L_4**–**L_6**. A 233.7 mg portion of pale yellow solid was isolated with yield 91.2%. IR (KBr, cm^{-1}): 3079.8 (w, NH), 2136.4 (s, CO), 2071.5 (s, CO), 2005.2 (m, CO), 1759.9 (m, *COO*), 1683.4 (m, CONH), 1608.7 (m, pyridine C=C), 1541.5 (m, Ar C=C). ^1H NMR ($CDCl_3$, TMS, ppm): δ 9.184 (s, 1H, NH), 8.831 (s, 1H, Ar–H), 8.575 (d, 1H, $J=8.0$ Hz, Ar–H), 8.517 (d, 1H, $J=5.2$ Hz, Ar–H), 7.884 (d, 1H, $J=7.2$ Hz, Ar–H), 7.564 (t, 1H, $J=7.6$ Hz, Ar–H), 7.478 (t, 1H, $J=6.8$ Hz, Ar–H), 7.376 (t, 1H, $J=7.6$ Hz, Ar–H), 7.208 (d, 1H, $J=8.4$ Hz, Ar–H), 2.418 (s, 3H, CH_3). ^{13}C NMR ($CDCl_3$, TMS, ppm): δ 196.8 (Ru–CO), 195.5 (Ru–CO), 171.2 (COO), 168.3 (CON), 157.1, 145.1, 143.6, 135.3, 134.4, 128.0, 127.6, 122.9, 117.8, 116.8, 116.6, 21.3. ESI-MS: calcd for $C_{17}H_{13}O_6Cl_2N_2Ru$ $[M+H]^+$ 512.9194, found 512.9106. Elemental Anal. Calcd for $C_{17}H_{12}N_2O_6Cl_2Ru$: C, 39.86; H, 2.36; N, 5.47%. Found: C, 40.03; H, 2.68; N, 5.35%.

4.10.20. Preparation of $[Ru(CO)_3Cl_2$-**L_5**$]$ (**12**)

A 228.9 mg portion of pale yellow solid was isolated with yield 89.4%. IR (KBr, cm^{-1}): 3324.6 (w, NH), 2137.5 (s, CO), 2064.9 (s, CO), 1996.0 (s, CO), 1715.6 (m, *COO*), 1616.4 (s, *CO*NH), 1593.1 (m, pyridine, C=C), 1513.2 (s, Ar C=C). ^1H NMR (DMSO-d_6, TMS, ppm): δ 11.275 (s, 1H, NH), 8.805 (m, 2H, pyridine $H_{2,6}$), 8.644 (d, 1H, $J=5.2$ Hz, Ar–H_6), 8.463 (d, 1H, $J=6.0$ Hz, Ar–H_3), 7.972 (d, 1H, $J=5.2$ Hz, Ar–H_4), 7.781 (m, 2H, pyridine $H_{3,5}$), 7.715 (d, 1H, $J=6.0$ Hz, Ar–H_5), 2.201 (s, CH_3). ^{13}C NMR (DMSO-d_6, TMS, ppm): δ 195.9 (Ru–CO), 194.3 (Ru–CO), 174.1 (COO), 167.0 (CON), 157.1, 149.0, 143.3, 134.1, 129.8, 121.5, 120.1, 118.9, 116.7, 21.4. ESI-MS: calcd for $C_{17}H_{13}O_6Cl_2N_2Ru$ $[M+H]^+$ 512.9194, found 512.9114. Elemental Anal. Calcd for $C_{17}H_{12}N_2O_6Cl_2Ru$: C, 39.86; H, 2.36; N, 5.47%. Found: C, 40.06; H, 2.49; N, 5.66%.

4.10.21. Preparation of $[Ru(CO)_3Cl_2$-**L_6**$]$ (**13**)

A 273.9 mg portion of yellow solid was isolated with yield 92.9%. IR (KBr, cm^{-1}): 3069.2 (w, NH_2), 2132.2 (v, CO), 2059.7 (v, CO), 1994.2 (s, CO), 1746.9 (m, *COO*), 1611.4 (s, *CO*NH), 1543.6 (m, pyridine, C=C), 1486.2 (s, Ar C=C). ^1H NMR ($CDCl_3$, TMS, ppm): δ 9.313 (s, NH), 8.222 (s, Ar–H), 8.084 (s, Ar–H), 7.949 (s, Ar–H), 7.857 (t, $J=6.8$ Hz, Ar–H), 7.545 (m, Ar–H), 7.130 (t, $J=8.4$ Hz, Ar–H), 6.998 (s, Ar–H), 6.926 (d, $J=7.6$ Hz, Ar–H), 5.251 (t, 1H, Bp–CH), 4.644 (t, 1H, Bp–CH), 2.337 (s, CH_3). ^{13}C NMR ($CDCl_3$, TMS, ppm): δ 197.3 (Ru–CO), 194.5 (Ru–CO), 173.9 (*COO*), 170.6 (*CO*N), 160.3, 158.7, 157.9, 148.1, 135.7, 134.3, 127.1, 125.6, 123.4, 122.1, 119.0, 45.1, 22.1. ESI-MS: calcd for $C_{18}H_{15}O_6Cl_2N_2Ru$ $[M+H]^+$ 526.9351, found 526.9256. Elemental Anal. Calcd for $C_{18}H_{14}N_2O_6Cl_2Ru$: C, 41.08; H, 2.68; N, 5.32%. Found: C, 41.71; H, 2.95; N, 5.43%.

4.10.22. Preparation of $[Ru(CO)_3$-**L_7**$]^+Cl^-$ (**14**)

$[Ru(CO)_3Cl_2]_2$ (256.0 mg, 0.50 mmol) was added to the solution of 164.1 mg (1.00 mmol) **L_7** and 200 μl (1.43 mmol) Et_3N in 15 ml of deoxygenated 1,2-dimethoxyethane. Then the solution was heated at 60 °C, and the mixture was stirred for 5 h in the presence of nitrogen atmosphere. The solvent was removed under vacuum, and the residue was extracted by minimum amount of THF. After filtering, the THF was removed and 322.6 mg golden yellow solid was obtained with yield 92.7%. IR (KBr, cm^{-1}) 2981.8 (w, NH_2), 2047.1 (v, CO), 1971.1 (v, CO), 1930.7 (m, CO), 1618.4 (s, C=N), 1448.0 (m, Ar C=C). ^1H NMR ($CDCl_3$, TMS, ppm): δ 9.099 (bs, 2H, NH_2), 8.346 (s, 1H, Ar–CH), 7.234–6.337 (m, Ar–H), 4.891 (d, 1H, $J=9.6$ Hz, NCH), 4.512 (d, 1H, $J=6.4$ Hz, NCH), 4.310 (d, 1H, $J=6.8$ Hz, NCH), 4.066 (d, 1H, $J=9.6$ Hz, N-CH). ^{13}C NMR ($CDCl_3$, TMS, ppm): δ 195.0 (Ru–CO), 188.3 (Ru–CO), 185.4 (Ru–CO), 161.9, 157.4, 133.2, 131.6, 125.3, 120.4, 115.2, 54.1, 39.61. Elemental Anal. Calcd for $C_{12}H_{11}N_2O_4RuCl$: C, 37.56; H, 2.89; N, 7.30%. Found: C, 37.98; H, 3.02; N, 7.46%.

4.10.23. Preparation of $[Ru(CO)_3$-**L_8**$]^+Cl^-$ (**15**)

Complex **15** was synthesized following the same procedure as for complex **14**, but changing the ligand **L_8**, 336.4 mg scarlet red solid was obtained with yield 90.9%. IR (KBr, cm^{-1}): 2049.3 (s, CO), 2022.2 (s, CO), 1973.8 (s, CO), 1935.1 (s, CO), 1611.9 (s, C=N), 1522.5 (m, pyridine C=C), 1466.8 (m, pyridine C=C), 1440.1 (m, Ar C=C). ^1H NMR ($CDCl_3$, TMS, ppm): δ 9.202 (s, Ar–CH), 7.346–6.557 (m, aromatic H). ^{13}C NMR ($CDCl_3$, TMS, ppm): δ 195.2 (Ru–CO), 188.0 (Ru–CO), 186.1 (Ru–CO), 173.1, 166.2, 156.8, 150.3, 139.2, 133.1, 131.8,

121.9, 117.4, 115.6. Elemental Anal. Calcd for $C_{15}H_9N_2O_4ClRu$: C, 43.12; H, 2.17; N, 6.71%. Found: C, 43.59; H, 2.32; N, 7.02%.

4.10.24. Preparation of [NEt$_4$][MCl(CO)$_5$] (M = Cr, Mo, W) [62]

Tetraethyl ammonium chloride (0.5 g) was heated with an excess (1 g) of M(CO)$_6$ (M = Cr, Mo, W) in diethylene glycol ether at 120 °C until the steady evolution of carbon monoxide ceased. The mixture was filtered hot under an atmosphere of nitrogen. Adding light petroleum to the cooled filtrate gave yellow crystals of the product. After removal of the excessive solvent by decantation, the crystals were rapidly washed with light petroleum, and the excess of solvent was removed at reduced pressure.

*4.10.25. Preparation of Cr(CO)$_5$ (η^1-NH$_2$CH$_2$COOCH$_3$) (**16**) [22]*

[NEt$_4$][CrCl(CO)$_5$] (0.4952 g, 1.387 mmol) dissolved in 15 ml dry dichloromethane. Glycine methyl ester hydrochloride salt (0.3512 g, 3.31 mmol) was neutralized by sodium carbonate in dichloromethane. The CH_2Cl_2 solution of free glycine methyl ester was added by syringe under ice-bath condition. In 2 h later, the ice-bath was removed and the reaction was stirred at 20 °C for 4 h until no more product formed. The CH_2Cl_2 was removed under vacuum, and the crude product purified by flash column chromatography on silica gel. Cr(CO)$_5$ (η^1-NH$_2$CH$_2$COOCH$_3$) as a yellow solid (yield 264.87 mg, 43.70%). IR (KBr, cm^{-1}): 3338.3 (m, NH$_2$), 3294.7 (m, NH$_2$), 2069.4 (s, CO), 1981.0 (s, CO), 1978.4 (v, CO), 1904.6 (v, CO), 1731.1 (v, *COO*). ^{1}H NMR (CDCl$_3$, TMS, ppm): δ 3.797 (s, 3H, OCH$_3$), 3.350 (s, 2H, CH$_2$), 2.117 (br, 2H, NH$_2$). ^{13}C NMR (CDCl$_3$, TMS, ppm): δ 220.6 (trans-CO), 216.9 (cis-CO), 172.5, 65.0, 54.6. ESI-MS: calcd for $CrC_8H_7NO_7Na$ $[M+Na]^+$ 303.9525, found 304.0754. Elemental Anal. Calcd for $CrC_8H_7NO_7$: C, 34.18; H, 2.51; N, 4.98%. Found: C, 34.34; H, 2.31; N, 4.75%.

*4.10.26. Preparation of Mo(CO)$_5$(η^1-NH$_2$CH$_2$COOCH$_3$) (**17**)*

Mo(CO)$_5$(η^1-NH$_2$CH$_2$COOCH$_3$) as a yellow solid 0.0871 g, yield 22.96%. R_f = 0.5 (CH_2Cl_2); IR (KBr, cm^{-1}): 3338.0 (m, NH$_2$), 3291.4 (m, NH$_2$), 2075.7 (m, CO), 1982.4 (s, CO), 1904.6 (v, CO), 1728.2 (m, COO). ^{1}H NMR (CDCl$_3$, TMS, ppm): δ 3.809 (s, 3H, OCH$_3$), 3.491 (t, 2H, NCH$_2$), 2.592 (br, 2H, NH$_2$). ^{13}C NMR (CDCl$_3$, TMS, ppm): δ 200.2 (trans-CO), 196.9 (cis-CO), 172.3, 64.7, 54.8. ESI-MS: calcd for $MoC_8H_7NO_7Na$ $[M+Na]^+$ 349.9174, found 349.9303. Elemental Anal. Calcd for $MoC_8H_7NO_7$: C, 29.56; H, 2.17; N, 4.31%. Found: C, 29.73; H, 2.29; N, 4.39%.

*4.10.27. Preparation of W(CO)$_5$(η^1-NH$_2$CH$_2$COOCH$_3$) (**18**)*

The procedure and workup were the same as that of **16**. W(CO)$_5$(η^1-NH$_2$CH$_2$COOCH$_3$) as a yellow solid 0.0871 g, yield 22.96%. R_f = 0.5 (CH_2Cl_2); IR (KBr, cm^{-1}): 3330.8 (m, NH$_2$), 3283.8 (m, NH$_2$), 2073.4 (m, CO), 2054 (s, CO), 1908.8 (v, CO), 1728.6 (m, COO). ^{1}H NMR (CDCl$_3$, TMS, ppm): δ 3.767 (s, 3H, OCH$_3$), 3.630 (t, 2H, J = 7.2 Hz, C*H*$_2$NH$_2$), 2.996 (br, 2H, NH$_2$). ^{13}C NMR (CDCl$_3$): δ 200.6 (trans-CO), 197.8 (cis-CO), 171.8, 64.0, 55.1. ESI-MS: calcd for $WC_8H_7NO_7Na$ $[M+Na]^+$ 435.9630, found 435.9621. Elemental Anal. Calcd for $WC_8H_7NO_7$: C, 23.27; H, 1.71; N, 3.39%. Found: C, 23.10; H, 1.84; N, 3.46%.

*4.10.28. Preparation of Cr(CO)$_5$(N-methyl imidazole) (**19**)*

[NEt$_4$][CrCl(CO)$_5$] (0.6039 g, 1.69 mmol) dissolved in 15 ml dry CH_2Cl_2. 200 μl *N*-methyl imidazole was added by syringe under ice-bath condition. In 2 h later, the ice-bath was removed and the reaction was stirred at 20 °C for 4 h until no more product formed. The CH_2Cl_2 was removed under vacuum, and the crude product purified by flash column chromatography on silica gel. 419.5 mg yellow solid was obtained with yield 69.54%. R_f = 0.9 (CH_2Cl_2). IR (KBr, cm^{-1}): 2065.9 (m, CO), 1983.0 (s, CO), 1914.8 (v, CO), 1885.2 (v, CO), 1867.6 (v, CO), 1531.3 (m, C=N). ^{1}H NMR (CDCl$_3$, TMS, ppm): δ 7.388 (s, 1H, N–CH=N), 7.264 (s, 1H, CH=N), 6.860 (s, 1H, CH=N), 3.693 (s, 3H, CH$_3$). ^{13}C NMR (CDCl$_3$, TMS, ppm): δ 215.5 (trans-CO), 203.7 (cis-CO), 136.2, 128.5, 120.7, 36.6. ESI-MS: calcd for $CrC_9H_7N_2O_5$ $[M+H]^+$ 274.9760, found 275.0953. Elemental Anal. Calcd for $CrC_9H_6N_2O_5$: C, 39.43; H, 2.21; N, 10.22%. Found: C, 39.52; H, 2.35; N, 10.09%.

*4.10.29. Preparation of Mo(CO)$_5$(N-methyl imidazole) (**20**)*

Mo(CO)$_5$(*N*-methyl imidazole) as a yellow solid (yield 33.20%, 193.8 mg). IR (KBr, cm^{-1}): 2006.2 (m, CO), 1986.4 (s, CO), 1914.4 (v, CO), 1889.9 (v, CO), 1862.9 (v, CO), 1531.7 (m, C=N). ^{1}H NMR (CDCl$_3$, TMS, ppm): δ 7.472 (s, 1H, N–CH=N), 6.963 (d, 1H, CH=N), 6.866 (d, 1H, CH=N), 3.681 (s, 3H, CH$_3$). ^{13}C NMR (CDCl$_3$, TMS, ppm): δ 214.52 (trans-CO), 202.9 (cis-CO), 135.8, 127.5, 121.7, 36.1. ESI-MS: calcd for $MoC_9H_6N_2O_5Na$ $[M+Na]^+$ 342.9228, found 342.9410. Elemental Anal. Calcd for $MoC_9H_6N_2O_5$: C, 33.98; H, 1.90; N, 8.81%. Found: C, 34.26; H, 1.97; N, 8.72%.

*4.10.30. Preparation of W(CO)$_5$(N-methyl imidazole) (**21**)*

W(CO)$_5$(*N*-methyl imidazole) as a yellow solid (yield 193.8 mg, 33.20%). R_f = 0.9 (CH_2Cl_2). IR (KBr, cm^{-1}): 2001.7 (m, CO), 1981.0 (s, CO), 1916.8 (v, CO), 1844.8 (v, CO), 1790.6 (v, CO), 1535.6 (m, C=N). ^{1}H NMR (CDCl$_3$, TMS, ppm): δ 7.304 (s, 1H, N–CH=N), 7.069 (s, 1H, CH=N), 6.772 (s, 1H, CH=N), 3.740 (s, 3H, CH$_3$). ^{13}C NMR (CDCl$_3$, TMS, ppm): δ 214.8 (trans-CO), 202.8 (cis-CO), 136.4, 128.5, 120.7, 37.2. ESI-MS: calcd for $WC_9H_7N_2O_5$ $[M+H]^+$ 406.9864, found 406.9850. Elemental Anal. Calcd for $WC_9H_6N_2O_5$: C, 26.63; H 1.49; N 6.90 %. Found: C, 26.51; H, 1.62; N, 6.98%.

Acknowledgments

This work was financially supported by the National Natural Science Foundations of China (No. 21171079) and Natural Science Foundations of Gansu province (No. 1107RJZA264).

Appendix A. Supplementary data

Supplementary data associated with this article can be found in the online version, at http://dx.doi.org/10.1016/j.ejmech.2013.12.041. These data include MOL files and InChIKeys of the most important compounds described in this article.

References

[1] L.E. Otterbein, Carbon monoxide: innovative anti-inflammatory properties of an age-old gas molecule, Antioxid. Redox Signal. 4 (2002) 309–319.
[2] S.W. Ryter, J. Alam, A.M.K. Choi, Heme oxygenase-1/carbon monoxide: from basic science to therapeutic applications, Physiol. Rev. 86 (2006) 583–650.
[3] A. Hoetzel, R. Schmidt, Carbon monoxide – poison or potential therapeutic? Der Anaesthesist 55 (2006) 1068–1079.
[4] B.E. Mann, CO-releasing molecules: a personal view, Organometallics 31 (2012) 5728–5735.
[5] T.R. Johnson, B.E. Mann, J.E. Clark, R. Foresti, C.J. Green, R. Motterlini, Metal carbonyls: a new class of pharmaceuticals? Angew. Chem. Int. Ed. 42 (2003) 3722–3729.
[6] R. Motterlini, P. Sawle, J. Hammad, S. Bains, R. Alberto, R. Foresti, C.J. Green, CORM-A1: a new pharmacologically active carbon monoxide-releasing molecule, FASEB J. 19 (2005) 284–286.
[7] R. Alberto, R. Motterlini, Chemistry and biological activities of CO-releasing molecules (CORMs) and transition metal complexes, Dalton Trans. 17 (2007) 1651–1660.
[8] T.S. Pitchumony, B. Spingler, R. Motterlini, R. Alberto, Syntheses, structural characterization and CO releasing properties of boranocarbonate $[H_3BCO_2H]^-$ derivatives, Org. Biomol. Chem. 8 (2010) 4849–4854.
[9] R. Motterlini, B.E. Mann, T.R. Johnson, J.E. Clark, R. Foresti, C.J. Green, Bioactivity and pharmacological actions of carbon monoxide-releasing molecules, Curr. Pharm. Des. 9 (2003) 2525–2539.
[10] B.E. Mann, R. Motterlini, CO and NO in medicine, Chem. Commun. 41 (2007) 4197–4208.
[11] R. Motterlini, L.E. Otterbein, The therapeutic potential of carbon monoxide, Nat. Rev. Drug Discov. 9 (2010) 728–743.

[12] R. Motterlini, J.E. Clark, R. Foresti, P. Sarathchandra, B.E. Mann, C.J. Green, Carbon monoxide-releasing molecules characterization of biochemical and vascular activities, Circ. Res. 90 (2002) e17–e24.

[13] T.R. Johnson, B.E. Mann, I.P. Teasdale, H. Adams, R. Foresti, C.J. Green, R. Motterlini, Metal carbonyls as pharmaceuticals? $[Ru(CO)_3Cl(glycinate)]$, a CO-releasing molecule with an extensive aqueous solution chemistry, Dalton Trans. 15 (2007) 1500–1508.

[14] R. Motterlini, B.E. Mann, R. Foresti, Therapeutic applications of carbon monoxide-releasing molecules, Expert Opin. Investig. Drugs 14 (2005) 1305–1318.

[15] S. Romanski, B. Kraus, U. Schatzschneider, J.M. Neudörfl, S. Amslinger, H.G. Schmalz, Acyloxybutadiene iron tricarbonyl complexes as enzyme-triggered CO-releasing molecules (ET-CORMs), Angew. Chem. Int. Ed. 50 (2011) 2392–2396.

[16] J. Niesel, A. Pinto, H.W.P. N'Dongo, K. Merz, I. Ott, R. Gust, U. Schatzschneider, Photoinduced CO release, cellular uptake and cytotoxicity of a tris(pyrazolyl) methane manganese tricarbonyl complex, Chem. Commun. 15 (2008) 1798–1800.

[17] H. Pfeiffer, A. Rojas, J. Niesel, U. Schatzschneider, Sonogashira and "Click" reactions for the N-terminal and side-chain functionalization of peptides with $[Mn(CO)_3(tpm)]^+$-based CO releasing molecules (tpm = tris(pyrazolyl) methane), Dalton Trans. 22 (2009) 4292–4298.

[18] R.D. Rimmer, H. Richter, P.C. Ford, A photochemical precursor for carbon monoxide release in aerated aqueous media, Inorg. Chem. 49 (2009) 1180–1185.

[19] U. Schatzschneider, Photoactivated biological activity of transition-metal complexes, Eur. J. Inorg. Chem. 10 (2010) 1451–1467.

[20] C.S. Jackson, S. Schmitt, Q.P. Dou, J.J. Kodanko, Synthesis, characterization, and reactivity of the stable Iron carbonyl complex $[Fe(CO)(N_4Py)](ClO_4)_2$: photo-activated carbon monoxide release, growth inhibitory activity, and peptide ligation, Inorg. Chem. 50 (2011) 5336–5338.

[21] R. Foresti, J. Hammad, J.E. Clark, T.R. Johnson, B.E. Mann, A. Friebe, C.J. Green, R. Motterlini, Vasoactive properties of CORM-3, a novel water-soluble carbon monoxide-releasing molecule, Br. J. Pharmacol. 142 (2004) 453–460.

[22] W.Q. Zhang, A.C. Whitwood, I.J.S. Fairlamb, J.M. Lynam, Group 6 carbon monoxide-releasing metal complexes with biologically-compatible leaving groups, Inorg. Chem. 49 (2010) 8941–8952.

[23] L. Hewison, T.R. Johnson, B.E. Mann, A.J.H.M. Meijer, P. Sawle, R. Motterlini, A re-investigation of $[Fe(l\text{-cysteinate})_2(CO)_2]^{2-}$: an example of non-heme CO coordination of possible relevance to CO binding to ion channel receptors, Dalton Trans. 40 (2011) 8328–8334.

[24] V.P.L. Velasquez, T.M.A. Jazzazi, A. Malassa, H. Goerls, G. Gessner, S.H. Heinemann, M. Westerhausen, Derivatives of photosensitive CORM-S1-CO complexes of iron and ruthenium with the $(OC)_2M(S\text{-}C\text{-}C\text{-}NH_2)_2$ fragment, Eur. J. Inorg. Chem. 2012 (2012) 1072–1078.

[25] W.Q. Zhang, A.J. Atkin, I.J.S. Fairlamb, A.C. Whitwood, J.M. Lynam, Synthesis and reactivity of molybdenum complexes containing functionalized alkynyl ligands: a photochemically activated CO-releasing molecule (PhotoCO-RM), Organometallics 30 (2011) 4643–4654.

[26] A.R. Marques, L. Kromer, D.J. Gallo, N. Penacho, S.S. Rodrigues, J.D. Seixas, G.J.L. Bernardes, P.M. Reis, S.L. Otterbein, R.A. Ruggieri, A.S.G. Goncalves, A.M.L. Goncalves, M.N. De Matos, I. Bento, L.E. Otterbein, W.A. Blättler, C.C. Romão, Generation of carbon monoxide releasing molecules (CO-RMs) as drug candidates for the treatment of acute liver injury: targeting of CO-RMs to the liver, Organometallics 31 (2012) 5810–5822.

[27] I.J.S. Fairlamb, A.K. Duhme-Klair, J.M. Lynam, B.E. Moulton, C.T. O'Brien, P. Sawle, J. Hammad, R. Motterlini, η^4-Pyrone iron(0)carbonyl complexes as effective CO-releasing molecules (CO-RMs), Bioorg. Med. Chem. Lett. 16 (2006) 995–998.

[28] I.J.S. Fairlamb, J.M. Lynam, B.E. Moulton, I.E. Taylor, A.K. Duhme-Klair, P. Sawle, R. Motterlini, η^1-2-Pyrone metal carbonyl complexes as CO-releasing molecules (CO-RMs): a delicate balance between stability and CO liberation, Dalton Trans. 33 (2007) 3603–3605.

[29] P. Sawle, J. Hammad, I.J.S. Fairlamb, B. Moulton, C.T. O'Brien, J.M. Lynam, A.K. Duhme-Klair, R. Foresti, R. Motterlini, Bioactive properties of iron-containing carbon monoxide-releasing molecules, J. Pharmacol. Exp. Ther. 318 (2006) 403–410.

[30] D. Scapens, H. Adams, T.R. Johnson, B.E. Mann, P. Sawle, R. Aqil, T. Perrior, R. Motterlini, $[(\eta\text{-}C_5H_4R)Fe(CO)_2X]$, X = Cl, Br, I, NO_3, CO_2Me and $[(\eta\text{-}C_5H_4R)Fe(CO)_3]^+$, R = $(CH_2)nCO_2Me$ (n = 0–2), and $CO_2CH_2CH_2OH$: a new group of CO-releasing molecules, Dalton Trans. 43 (2007) 4962–4973.

[31] W.Q. Zhang, A.J. Atkin, R.J. Thatcher, A.C. Whitwood, I.J.S. Fairlamb, J.M. Lynam, Diversity and design of metal-based carbon monoxide-releasing molecules (CO-RMs) in aqueous systems: revealing the essential trends, Dalton Trans. 22 (2009) 4351–4358.

[32] L. Hewison, S.H. Crook, T.R. Johnson, B.E. Mann, H. Adams, S.E. Plant, P. Sawle, R. Motterlini, Iron indenyl carbonyl compounds: CO-releasing molecules, Dalton Trans. 39 (2010) 8967–8975.

[33] M.A. Gonzalez, N.L. Fry, R. Burt, R. Davda, A. Hobbs, P.K. Mascharak, Designed iron carbonyls as carbon monoxide (CO) releasing molecules: rapid CO release and delivery to myoglobin in aqueous buffer, and vasorelaxation of mouse aorta, Inorg. Chem. 50 (2011) 3127–3134.

[34] R. Kretschmer, G. Gessner, H. Görls, S.H. Heinemann, M. Westerhausen, Dicarbonyl-bis(cysteamine) iron(II): a light induced carbon monoxide releasing molecule based on iron (CORM-S1), Inorg. Biochem. 105 (2011) 6–9.

[35] A.J. Atkin, I.J.S. Fairlamb, J.S. Ward, J.M. Lynam, CO release from norbornadiene iron(0) tricarbonyl complexes: importance of ligand dissociation, Organometallics 31 (2012) 5894–5902.

[36] L.S. Nobre, J.D. Seixas, C.C. Romão, L.M. Saraiva, Antimicrobial action of carbon monoxide-releasing compounds, Antimicrob. Agents Chemother. 51 (2007) 4303–4307.

[37] P.C. Kunz, W. Huber, A. Rojas, U. Schatzschneider, B. Spingler, Tricarbonylmanganese(I) and -rhenium(I) complexes of imidazol-based phosphane ligands: influence of the substitution pattern on the CO release properties, Eur. J. Inorg. Chem. 35 (2009) 5358–5366.

[38] N.E. Brückmann, M. Wahl, G.J. Reiss, M. Kohns, W. Wätjen, P.C. Kunz, Polymer conjugates of photoinducible CO-releasing molecules, Eur. J. Inorg. Chem. 29 (2011) 4571–4577.

[39] S.H. Crook, B.E. Mann, A.J.H.M. Meijer, H. Adams, P. Sawle, D. Scapens, R. Motterlini, $[Mn(CO)_4\{S_2CNMe(CH_2CO_2H)\}]$, a new water-soluble CO-releasing molecule, Dalton Trans. 40 (2011) 4230–4235.

[40] M.A. Gonzalez, M.A. Yim, S. Cheng, A. Moyes, A.J. Hobbs, P.K. Mascharak, Manganese carbonyls bearing tripodal polypyridine ligands as photoactive carbon monoxide-releasing molecules, Inorg. Chem. 51 (2012) 601–608.

[41] G. Dördelmann, H. Pfeiffer, A. Birkner, U. Schatzschneider, Silicium dioxide nanoparticles as carriers for photoactivatable CO-releasing molecules (PhotoCORMs), Inorg. Chem. 50 (2011) 4362–4367.

[42] W. Huber, R. Linder, J. Niesel, U. Schatzschneider, B. Spingler, P.C. Kunz, A comparative study of tricarbonylmanganese photoactivatable CO releasing molecules (PhotoCORMs) by using the myoglobin assay and time-resolved IR spectroscopy, Eur. J. Inorg. Chem. 19 (2012) 3140–3146.

[43] F. Mohr, J. Niesel, U. Schatzschneider, C.W. Lehmann, Synthesis, structures, and CO releasing properties of two tricarbonyl manganese(I) complexes, Z. Anorg. Allg. Chem. 638 (2012) 543–546.

[44] F. Zobi, A. Degonda, M.C. Schaub, A.Y. Bogdanova, CO releasing properties and cytoprotective effect of cis-trans-$[Re^{II}(CO)_2Br_2L_2]_n$ complexes, Inorg. Chem. 49 (2010) 7313–7322.

[45] F. Zobi, O. Blacque, Reactivity of 17 e^- complex $[Re^{II}Br_4(CO)_2]^{2-}$ with bridging aromatic ligands, characterization and CO-releasing properties, Dalton Trans. 40 (2011) 4994–5001.

[46] F. Zobi, O. Blacque, R.A. Jacobs, M.C. Schaub, A.Y. Bogdanova, 17e^- rhenium dicarbonyl CO-releasing molecules on a cobalamin scaffold for biological application, Dalton Trans. 41 (2012) 370–378.

[47] D.E. Bikiel, E.G. Solveyra, F. Di Salvo, H.M.S. Milagre, M.N. Eberlin, R.S. Correa, J. Ellena, D.A. Estrin, F. Doctorovich, Tetrachlorocarbonyliridates: water-soluble carbon monoxide releasing molecules rate-modulated by the sixth ligand, Inorg. Chem. 50 (2011) 2334–2345.

[48] K.S. Davidge, G. Sanguinetti, C.H. Yee, B.E. Mann, R. Motterlini, R.K. Poole, Carbon monoxide-releasing antibacterial molecules target respiration and global transcriptional regulators, J. Biol. Chem. 284 (2009) 4516–4524.

[49] K. Meister, J. Niesel, U. Schatzschneider, N. Metzler-Nolte, D.A. Schmidt, M. Havenith, Label-free imaging of metal-carbonyl complexes in live cells by Raman microspectroscopy, Angew. Chem. Int. Ed. 49 (2010) 3310–3312.

[50] T. Santos-Silva, A. Mukhopadhyay, J.D. Seixas, G.J.L. Bernardes, C.C. Romão, M.J. Romão, CORM-3 reactivity toward proteins: the crystal structure of a Ru(II) dicarbonyl–lysozyme complex, J. Am. Chem. Soc. 133 (2011) 1192–1195.

[51] M.F.A. Santos, J.D. Seixas, A.C. Coelho, A. Mukhopadhyay, P.M. Reis, M.J. Romão, C.C. Romão, T. Santos-Silva, New insights into the chemistry of *fac*-$[Ru(CO)_3]^{2+}$ fragments in biologically relevant conditions: the CO releasing activity of $[Ru(CO)_3Cl_2(1,3\text{-thiazole})]$, and the X-ray crystal structure of its adduct with lysozyme, J. Inorg. Biochem. 117 (2012) 285–291.

[52] H. Smith, B.E. Mann, R. Motterlini, R.K. Poole, The carbon monoxide-releasing molecule, CORM-3 $[Ru(CO)_3Cl(glycinate)]$, targets respiration and oxidases in campylobacter jejuni, generating hydrogen peroxide, IUBMB Life 63 (2011) 363–371.

[53] A.J. Atkin, J.M. Lynam, B.E. Moulton, P. Sawle, R. Motterlini, N.M. Boyle, M.T. Pryce, I.J.S. Fairlamb, Modification of the deoxy-myoglobin/carbonmonoxy-myoglobin UV–vis assay for reliable determination of CO-release rates from organometallic carbonyl complexes, Dalton Trans. 40 (2011) 5755–5761.

[54] M. Seveso, M. Vadori, E. Bosio, F. Fante, F. Besenzon, L. Ravarotto, S. Bedendo, T.R. Johnson, B.E. Mann, R. Motterlini, E. Cozzi, E. Ancona, Pharmacological effects and tolerability profile of a carbon monoxide-releasing molecule (CORM-3) in primates, Am. J. Transplant. 5 (2005) 306–307.

[55] E. Schlede, E. Genschow, H. Spielmann, G. Stropp, D. Kayser, Oral acute toxic class method: a successful alternative to the oral LD_{50} test, Regul. Toxicol. Pharmacol. 42 (2005) 15–23.

[56] R. Cini, S. Defazio, G. Tamasi, M. Casolaro, L. Messori, A. Casini, M. Morpurgo, M. Hursthouse, Fac-$\{Ru(CO)_3\}^{2+}$-core complexes and design of metal-based drugs. Synthesis, structure, and reactivity of Ru–thiazole derivative with serum proteins and absorption-release studies with acryloyl and silica hydrogels as carriers in physiological media, Inorg. Chem. 46 (2007) 79–92.

[57] N. Malek-Saied, R.E. Aissi, S. Ladeira, E. Benoist, Synthesis and biological evaluation of a novel ^{99m}Tc-cyclopentadienyltricarbonyl technetium complex as a new potential brain perfusion imaging agent, Appl. Organomet. Chem. 25 (2011) 680–686.

[58] T. Hashimoto, A. Endo, N. Nagao, G.P. Satô, K. Natarajan, K. Shimizu, Synthesis and characterization of sulfur-bridged binuclear β-diketonatoruthenium complexes and a monomeric ruthenium complex. Crystal and molecular structures of racemic and meso Isomers of $[Ru(acac)_2(\mu\text{-topd-}O, S,O')$

$Ru(acac)_2$] (acac = acetylacetonato and topd = 3-thioxo-2,4-pentanedione), Inorg. Chem. 37 (1998) 5211–5220.
[59] J.E. Clark, P. Naughton, S. Shurey, C.J. Green, T.R. Johnson, B.E. Mann, R. Foresti, R. Motterlini, Cardioprotective actions by a water-soluble carbon monoxide-releasing molecule, Circ. Res. 93 (2003) e2–e8.
[60] R. Motterlini, B.E. Mann, Therapeutic delivery of carbon monoxide: WIPO Patent No. 2002092075, 2002-11-22.
[61] M. Haukka, P. Hirva, S. Luukkanen, M. Kallinen, M. Ahlgrén, T.A. Pakkanen, Reactions of ruthenium bipyridine catalyst precursors: synthetic, structural, and theoretical studies on ruthenium mono(bipyridine) carbonyls in ethylene glycol solutions, Inorg. Chem. 38 (1999) 3182–3189.
[62] E.W. Abel, J.G. Reid, I.S. Butler, The anionic halogenopentacarbonyls of chromium, molybdenum, and tungsten, J. Chem. Soc. 382 (1963) 2068–2070.